Filling in gaps in *Clostridium thermocellum* metabolism through co-culturing with hydrogenotroph, *Methanothermobacter marburgensis*

by

Alyza Karen Eusebio

A thesis submitted to the Faculty of Graduate Studies of

The University of Manitoba

in partial fulfilment of the requirements for the degree of

MASTER OF SCIENCE

Department of Microbiology

University of Manitoba

Winnipeg

Copyright © 2022 by Karen Eusebio

ABSTRACT

Clostridium thermocellum is one of the most promising candidates for consolidated bioprocessing of lignocellulosic biomass to biofuels and chemicals but its low product yield and the presence of unexpected minor fermentation products, such as amino acids, has restricted industrial scale production. Few reports have compared the physiological effects of end-product accumulation and the behavior of *C. thermocellum* in a natural, consortium setting. This may provide a more detailed understanding of the complex metabolism of *C. thermocellum*, aiding future engineering efforts to increase product yield. In this study, we grew *C. thermocellum* in co-culture with *Methanothermobacter marburgensis*, a hydrogenotrophic methanogen, on cellulose in batch culture at 60 ºC to investigate the physiological effects of continuous H_2 removal on *C. thermocellum*. When grown in co-culture, minimal H_2 concentration and continuous CH_4 production was detected, indicating continuous H_2 and CO_2 consumption by *M. marburgensis*. *C. thermocellum* growth rate did not change significantly, but a faster rate of cellulose hydrolysis was observed. Major end-product profile of *C. thermocellum* changed with the most notable difference being an increase in acetate, and a decrease in formate and ethanol. Changes in alternate end-products, such as amino acids and TCA cycle intermediates, were also observed. The metabolic shift to H_2 and acetate in response to continuous H_2 removal was accompanied by changes in the expression of [FeFe] H_2ases of *C. thermocellum*: (a) 10-fold decrease in Cthe_0430, (b) 2-fold decrease in Cthe_0342, (c) 1.5-fold decrease in Cthe_3003. We demonstrated that growth with a naturally occurring hydrogenotrophic partner, such as methanogens, alter the metabolic patterns and H_2ase gene expression in *C. thermocellum*. Low H_2 partial pressure required to overcome thermodynamic barriers for the oxidation of reducing equivalents was achieved by continuous H_2 removal via methanogen consumption.

ACKNOWLEDGEMENTS

Thank you to my supervisor, Dr. Richard Sparling, for giving me this opportunity and for being the best cheerleader during this journey. I appreciate your patience and support. Also thank you to my committee members, Dr. David Levin and Dr. Deborah Court, for your valuable scientific inputs and encouragement during the past few years.

I will forever be grateful for my lab members, past and present: Alan Froese, Steve Daley and Jocelyn Plouffe. They have made this journey so much more enjoyable and I couldn't have asked for better lab mates. Thank you Alan for being the biggest help with my project and always answering my questions. Thank you Steve for always wheeling yourself over to my desk when I need to talk things through and going on coffee walks with me. Thank you Jocelyn for being as excited as me for free food and decorating our door.

I would also like to thank all the lovely people from the Microbiology department - my fellow grad students, admin ladies, prep room ladies, caretakers, and PIs. I was never turned down whenever I asked for help. Thank you to our honorary lab member, Ola Salama, for always checking on me in the lab and reminding me that my small baby steps will always add up. Thank you to Dr. Erwin Huebner for taking the time to train me on microscopy and Levin lab members for always helping me with troubleshooting the HPLC machine.

Lastly, I would like to thank my family and friends for being the greatest support system. I wouldn't have gotten this far without you.

DEDICATION

To my parents, Renante and Melgie, and my partner, Darren.

TABLE OF CONTENTS

ABSTRACT **2**

ACKNOWLEDGEMENTS **3**

DEDICATION **4**

TABLE OF CONTENTS **5**

LIST OF TABLES **7**

LIST OF FIGURES **8**

LIST OF ABBREVIATIONS **9**

Chapter 1: LITERATURE REVIEW **10**

1.1 Phasing out fossil fuels **10**

1.1.1 Impacts of fossil fuels 10

1.1.2 Help from biotechnology 11

1.1.3 The case for biofuels 11

1.2 Lignocellulosic fuels and chemicals **13**

1.2.1 Lignocellulose 13

1.2.2 Consolidated bioprocessing 14

1.2.3 Strategies to design ideal CBP microorganisms 15

1.2.4 Natively cellulolytic CBP candidates 16

1.3 *Clostridium thermocellum* **17**

1.3.1 Best candidate for CBP 17

1.3.2 Cellulose adherence and utilization 18

1.3.3 Atypical central metabolism 20

1.3.4 Mixed-product fermentation 25

1.3.5 Overflow metabolism 28

1.4 Filling in gaps **30**

1.4.1 Natural consortia 30

1.4.2 Targeting H_2 production in *C. thermocellum* 31

1.4.3 *Methanothermobacter marburgensis* 33

1.5 Research objectives **34**

Chapter 2: MATERIALS AND METHODS **35**

2.1 Microorganisms and Media **35**

2.2 Experimental Design **36**

2.3 End-product Analyses **36**

2.4 GC-MS Analysis for Additional End-products **37**

2.5 Residual cellulose **38**

2.6 DNA extraction and qPCR **39**
2.7 Scanning Electron Microscopy **40**
2.8 RNA Extraction and RT-qPCR **41**
2.9 Data analysis **43**
Chapter 3: RESULTS **45**
3.1 Growth parameters **45**
3.2 Fermentation end-products **49**
3.3 Alternate end-products at high carbon concentrations **54**
3.4 Cell interaction in co-culture **59**
3.5 H_2ase gene expression in *C. thermocellum* **63**
Chapter 4: DISCUSSION **65**
4.1 Growth and end-product synthesis of *C. thermocellum* in the presence and absence of *M. marburgensis* **65**
4.2 *C. thermocellum* and *M. marburgensis* interaction in co-culture **67**
4.3 H_2ase gene expression in *C. thermocellum* **69**
Chapter 5: CONCLUSION AND FUTURE DIRECTIONS **71**
APPENDIX **73**
REFERENCES **78**

LIST OF TABLES

Table 1. Primer and probe sequences used for cell enumeration. 40

Table 2. Primer sequences used for comparative quantification of H_2ase expression. 43

Table 3. Concentrations of fermentation end-products and residual cellulose, and calculated carbon balance and O/R index at the end of fermentation (40h) when cultures were grown with 2 g/L cellulose. 53

Table 4. Calculated carbon balance and O/R index in *C. thermocellum* monoculture and *C. thermocellum* and *M. marburgensis* co-culture grown with 2 g/L cellulose. 77

LIST OF FIGURES

Figure 1. Proposed central metabolic pathways of *C. thermocellum*..... 24
Figure 2. Mixed-product fermentation pathway in *C. thermocellum*. 28
Figure 3. Growth of *C. thermocellum* and *M. marburgensis* in co-culture (A), *C. thermocellum* in monoculture (B), and *M. marburgensis* in monoculture (C). 47
Figure 4. Cellulose hydrolysis (A) and pH (B) in *C. thermocellum* monoculture and *C. thermocellum* and *M. marburgensis* co-culture when grown with 2 g/L cellulose. 48
Figure 5. Detected concentrations of gases produced by *C. thermocellum* and *M. marburgensis* co-culture (A) and *C. thermocellum* monoculture (B), and calculated concentrations of gases produced by *C. thermocellum* in co-culture with *M. marburgensis* (C) when grown with 2 g/L cellulose. 51
Figure 6. Detected concentrations of organic end-products in *C. thermocellum* and *M. marburgensis* co-culture (A) and *C. thermocellum* monoculture (B) when grown with 2 g/L cellulose. 52
Figure 7. Detected concentrations of amino acids in *C. thermocellum* and *M. marburgensis* monocultures and co-culture at high carbon loading (10 g/L Avicel). 56
Figure 8. Detected concentrations of succinate, α-hydroxyglutarate, fumarate, and α-ketoglutarate in *C. thermocellum* and *M. marburgensis* monocultures and co-culture at high carbon loading (10 g/L Avicel). 57
Figure 9. Distribution of typical fermentation end-products (A), amino acids (B), and TCA cycle intermediates (C) at high initial carbon concentrations. 58
Figure 10. Distribution of *C. thermocellum* and *M. marburgensis* cells on cotton and in the supernatant during mid-exponential phase (24 h pi)..... 60
Figure 11. Representative SEM images of *C. thermocellum* and *M. marburgensis* monocultures and co-cultures grown on cotton threads. 62
Figure 12. Expression of H_2ase genes in *C. thermocellum* in co-culture with *M. marburgensis* relative to *C. thermocellum* in monoculture during the mid-exponential phase of growth (16 h pi) with 2 g/L of cellulose. 64
Figure 13. Gas consumption and production in *M. marburgensis* monoculture grown on minimal media with a mixture of 80% H_2 and 20% CO_2..... 73
Figure 14. *C. thermocellum* fermentation end-products in monoculture and co-culture with *M. marburgensis* at high carbon loading (10 g/L Avicel). 74
Figure 15. Gaseous end-products and pH in *C. thermocellum* monoculture (A), *C. thermocellum* + *M. marburgensis* co-culture (B), and *M. marburgensis* monoculture (C) on 2 g/L of untreated cotton..... 76

LIST OF ABBREVIATIONS

ATP/ADP/AMP: adenosine triphosphate/diphosphate/monophosphate

cDNA: complementary deoxyribonucleic acid

CO_2: carbon dioxide

DEPC: diethyl pyrocarbonate

DNA: deoxyribonucleic acid

EDTA: ethylenediaminetetraacetic acid

FADH: flavin adenine dinucleotide

Fd: ferredoxin

GTP/GDP: guanosine triphosphate/diphosphate

H_2: hydrogen gas

H_2ase: hydrogenase

MTBSTFA: *N*-Methyl-*N*-*tert*-butyldimethylsilyltrifluoroacetamide

MOPS: 3-(*N*-morpholino)propanesulfonic acid

NAD(P)H: nicotinamide adenine dinucleotide (phosphate)

PABA: *para*-aminobenzoic acid

PCR: polymerase chain reaction

PPi: inorganic pyrophosphate

Pi: inorganic phosphate

qPCR: quantitative polymerase chain reaction

RNA: ribonucleic acid

RT-qPCR: reverse transcription quantitative polymerase chain reaction

TBDMS: tert-butyldimethylsilyl

Chapter 1: LITERATURE REVIEW

1.1 Phasing out fossil fuels

1.1.1 Impacts of fossil fuels

The Industrial Revolution unlocked fossil fuels as a new energy source, which have become vital to how civilization is powered and significantly contributed to the economic development of many nations (Wrigley, 2013). The rapid increase in primary power consumption associated with the expansion of the human population has presented concerns relating to sustainability due to the environmental and human health impacts of fossil fuels. CO_2, along with other greenhouse gases (GHG), released from burning fossil fuels raises the infrared opacity of the Earth's atmosphere by trapping heat that would have otherwise been radiated out into space, resulting in the heating of the Earth (Hoffert et al., 2002). Anthropogenic climate change caused by the rapid heating of the Earth leads to rising sea levels and extremes in weather patterns. Climate change contributes to habitat loss and fragmentation, leading to increased extinction risk of many species and reduced global biodiversity (Bellard et al., 2012; Robillard et al., 2015). Extreme weather patterns induced by climate change, such as droughts and floods, may affect access to safe drinking water and could lead to food insecurity (Myers et al., 2014). Furthermore, rapid warming can affect insect vectors that carry pathogens and increase the risk of infectious illnesses (WHO, 2008). New applications of emerging technologies to help offload the global dependence on fossil fuels and reduce GHG emissions are needed to combat climate change and its negative impacts on the environment and human health.

1.1.2 Help from biotechnology

Technological processes using microbial fermentation can be traced as far back as 7000 BC with chemical analyses of ancient organics absorbed by pottery jars that contained a mixed fermented beverage of rice, honey, and fruit (McGovern et al., 2004). Today, microbial fermentations play an important role in the industrial production of biofuels and valuable chemicals for food and non-food industries, and can make significant contributions to reducing the global dependence on fossil fuels. Biofuels have emerged as a potentially major alternative to fossil fuels, especially for transport modes that are currently difficult to electrify (Solomon, 2010; Zhang & Fujimori, 2020). Synthesis of valuable chemicals (e.g. acetic acid, lactic acid, ethylene) via microbial fermentation does not rely on fossil fuel-derived precursors, unlike synthesis via chemical processes (Biddy et al., 2016; Mazzoli et al., 2020). Further studies of anaerobic microorganisms to advance our understanding of their metabolism could improve their industrial potential and biotechnological processes for the production of biofuels and valuable chemicals using renewable biomass sources.

1.1.3 The case for biofuels

The transportation sector is one of the largest contributors to GHG emissions, accounting for 14% of global GHG emissions (IPCC, 2014). GHG emissions from transportation are comprised mostly of CO_2 emitted from the combustion of gasoline and diesel to power the movement of people and goods via road, rail, air, and marine transportation. Biofuels are renewable sources of energy that can provide mitigation benefits in the short- and medium-term (Fulton et al., 2015). They have less GHG emissions than fossil fuels due to the uptake of CO_2 in the atmosphere during the growth of the biomass used for biofuel production. Ethanol is the most widely used biofuel worldwide and is the main focus of biofuel research (Solomon, 2010; Lynd et

al., 2017). Other potential biofuels include biodiesel, methanol, hydrogen, butanol, and dimethyl ether (Solomon, 2010).

Biofuels can be subdivided into three generations (first, second, and third) based on the type of biomass used. First-generation biofuels are derived from food or animal feed crops, such as corn, wheat, sugar cane, and palm oil (Jeswani et al., 2020). Second-generation biofuels, also known as lignocellulosic biofuels, are derived from lignocellulose, which is a component of non-food crops that originate from a large variety of sources (Jeswani et al., 2020). Third-generation biofuels are derived from microalgae (Chowdhury & Loganathan, 2019). Unlike first-generation biofuels, production techniques and pathways involved in second and third-generation biofuels are still in the research and development phase, hence they are often referred to as advanced biofuels (Jeswani et al., 2020).

Scaling-up the use of biofuels entails many challenges related to feedstock supply, land use, conversion technologies, and policies required to ensure sustainable production (Fulton et al., 2015; Souza et al., 2015). Production of first-generation biofuel feedstocks competes with other land uses and presents concerns such as increasing food insecurity, exacerbating deforestation, destroying ecosystems, and aggravating rural poverty (Zhang & Fujimori, 2020). As a result of the impracticality of biomasses for first-generation biofuels, scientists concentrated on second-generation biofuels as they can use non-food crops, which address issues of food competition and negative impacts on the environment associated with increased farming (Chowdhury & Loganathan, 2019). The conversion of lignocellulosic waste to fuels has potentially significant contributions to reducing GHG emissions, waste reduction, economic development, and enhancing the sustainability of agricultural landscapes (Prajapati et al., 2021). Despite the benefits of lignocellulosic biofuels, the feasibility of the bioconversion process is still a major challenge. This

is due to the high cost of pretreatment required to deconstruct lignocellulosic biomass, which is the key challenge to overcome for industrial-scale production of biofuels and biochemicals (Lynd et al., 2005).

1.2 Lignocellulosic fuels and chemicals

1.2.1 Lignocellulose

Lignocellulose makeup plant cell walls and can originate from dedicated energy crops (e.g. *Miscanthus*, switchgrass), agricultural residues (e.g. rice straw, corn stovers), forest residues (e.g. branches, foliage), and cellulosic waste (e.g. municipal and industrial solid wastes) (Parisutham et al., 2014; Jeswani et al., 2020). The major composition of lignocellulose consists of lignin, hemicellulose, and cellulose. Lignin is a heterogeneous polymer composed of phenyl propane subunits, and its interactions with hemicellulose and cellulose affect the recalcitrance of the biomass to biodegradation (Li et al., 2009). Hemicellulose is a heterogeneous polymer that has a composition that is plant species-specific and generally consists of pentoses, hexoses, and uronic acids with a highly branched backbone (Sun et al., 2016). As a result of its heterogeneous and branched nature, hemicellulose is not crystalline and is more readily accessible for hydrolysis compared to cellulose (Fellows et al., 2012). Cellulose is a linear, insoluble biopolymer composed of glucose subunits with β-1,4 linkages (Sun et al., 2016). Cellulose molecules aggregate into highly ordered structures through an extensive network of hydrogen bonds, resulting in a crystalline structure which limits access to enzymes for hydrolysis (Fellows et al., 2012). The presence of lignin and the crystalline structure of cellulose contributes to the recalcitrant nature of lignocellulose, making it difficult to fragment its major components and transform them into higher-value products (Parisutham et al., 2014).

1.2.2 Consolidated bioprocessing

Lignocellulosic biomass is the most abundant and low-cost substrate for renewable fuel and chemical production. The primary obstacle impeding the more widespread use of lignocellulosic biomass feedstocks is the high cost of pretreatment and exogenous enzyme supplementation associated with traditional ethanol production from yeast fermentation (Lynd et al., 2005). The general process configuration for lignocellulosic biofuel production via yeast fermentation is as follows: pretreatment, enzyme production, saccharification, and fermentation (Parisutham et al., 2014). Pretreatments are required to overcome the recalcitrant nature of lignocellulose and make polysaccharides easily accessible to enzymes for hydrolysis (Sun et al., 2016). Enzymatic saccharification and fermentation are also key determinants of the overall efficiency and sustainability of the conversion process (Parisutham et al., 2014). A better process would involve the use of microbes that could thrive efficiently on untreated or minimally treated lignocellulosic substrates, and are capable of simultaneous saccharification and fermentation.

Consolidated bioprocessing (CBP) combines enzyme production, enzymatic saccharification, and fermentation of the resulting sugars in a single-step process (Parisutham et al., 2014). This process offers reduced cost and higher efficiency as it avoids costs of capital, maintenance, substrate and other raw materials, and utilities associated with exogenous hydrolytic enzyme production (Lynd et al., 2005; Jouzani & Taherzadeh, 2015). It also avoids inhibition of cellulases by hydrolysis products, which is common in conventional systems but not in CBP, as they are transformed via fermentation and do not accumulate (Dashtban et al., 2009). Wild-type microorganisms that simultaneously and with high efficiency produce hydrolytic enzymes and transform sugars into valuable products are currently not available, but significant efforts have been given to discovering and engineering microorganisms for CBP applications (Lynd et al.,

2005). The development of CBP has been investigated increasingly in recent years for cost-competitive production of ethanol as biofuels but it is applicable to any fermentation product.

1.2.3 Strategies to design ideal CBP microorganisms

CBP technologies can combine enzyme production, saccharification, and fermentation in a single step via the application of a single microorganism or a consortium of microorganisms (Jouzani & Taherzadeh, 2015). There are two major strategies being used to generate ideal microorganisms for CBP applications. The recombinant cellulolytic strategy starts with non-cellulolytic microorganisms that possess desired product formation properties and engineers them to express enzymes to hydrolyze lignocellulose (Lynd et al., 2005). Additionally, industrial microbes, such as *Saccharomyces cerevisiae* and *Escherichia coli*, often do not metabolize other sugars in the presence of glucose due to carbon catabolite repression and need to be manipulated to express heterologous enzymes to expand soluble substrate utilization (Ha et al., 2011; Vinuselvi & Lee, 2012). Native cellulolytic strategy finds naturally cellulolytic microorganisms, such as *Clostridium* sp. and *Trichoderma reesei*, and aims to improve their product-related properties (Lynd et al., 2005; Jouzani & Taherzadeh, 2015). Co-culture systems may also be developed for CBP applications using saccharolytic and fermentative microorganisms that possess synergistic hydrolysis enzymes and metabolic capabilities (Froese et al., 2019).

The major constraints with cellulolytic microorganisms are that they are not as readily amenable to genetic manipulation and their physiology is not as well-understood compared to well-established industrial microbes (Parisutham et al., 2014). However, studies with *Clostridium* sp. have confirmed the feasibility of genetic manipulation to improve product yield in some cellulolytic microorganisms (Biswas et al., 2015; Tian et al., 2017). Developing ideal CBP microorganisms using the native cellulolytic strategy is more feasible due to the large and complex

variety of enzymes required to deconstruct lignocellulose, and the high energy consumption associated with protein secretion (Akinosho et al., 2014; Parisutham et al., 2014). This includes methodologies such as isolation and characterization of new strains (Kato et al., 2004), adaptive evolution (Holwerda et al., 2020; Yayo et al., 2021), or development of improved bioprocessing and fermentation systems (Blunt et al., 2015).

1.2.4 Natively cellulolytic CBP candidates

There are several wild-type fungi and bacteria with CBP capabilities. Cellulolytic fungi from various genera have been discovered to possess the ability to produce ethanol, such as *Trichoderma*, *Fusarium*, *Aspergillus*, and *Paecilomyces* (Jouzani & Taherzadeh, 2015). However, they only produce and secrete high amounts of cellulases under aerobic conditions while ethanol production occurs predominantly under anaerobic conditions (Xu et al., 2009). Mesophilic anaerobic bacteria capable of lignocellulose deconstruction can be used to create symbiotic co-culture systems with other mesophilic solventogenic microorganisms (Jouzani & Taherzadeh, 2015). A symbiotic co-culture of *Lachnoclostridium phytofermentans* (formerly *Clostridium phytofermentans* (Yutin & Galperin, 2013)) and fermenting yeasts, such as *Candida molischiana* and *S. cerevisiae*, can enhance substrate utilization and increase ethanol yield (Zuroff et al., 2013). Co-culture of *Clostridium acetobutylicum* and *Acetivibrio cellulolyticus* (formerly *Clostridium cellulolyticum* (Tindall, 2019)) have been confirmed to demonstrate cellulolytic and metabolic synergism resulting in higher butanol production (Salimi & Mahadevan, 2013).

Hyperthermophilic anaerobic bacteria from the genus *Caldicellulosiruptor* possess relatively high lignocellulose degradation abilities due to their high optimal growth temperatures ($\geq$80 ^{o}C) and synergistic multi-modular enzymes (Lee et al., 2020), and produce high amounts of H_2 (Yang et al., 2010). Thermophilic anaerobic bacteria represent the most promising candidates

for CBP, such as *Acetivibrio thermocellus* (formerly *Clostridium thermocellum* (Tindall, 2019)), *Acetivibrio clariflavus* (formerly *Clostridium clariflavum* (Tindall, 2019)), *Thermoclostridium stercorarium* (formerly *Clostridium stercorarium* (Zhang et al., 2018)), and *Geobacillus* sp. (Blumer-Schuette et al., 2014). Deconstruction of lignocellulose involves secreted free enzyme systems or multienzyme complexes, referred to as cellulosomes (Blumer-Schuette et al., 2014). *A. thermocellus* has emerged as an attractive high utility candidate for CBP due to its use of a cell wall-bound cellulosome that has demonstrated remarkable enzymatic hydrolysis efficiency (Lu et al., 2006). This thesis will focus on *A. thermocellus*, and how a more detailed understanding of its metabolism and interaction in a natural consortium setting may help to aid in the development of engineered strains for CBP applications.

1.3 *Clostridium thermocellum*

1.3.1 Best candidate for CBP

Clostridium thermocellum is one of the most well-characterized and promising candidates for CBP applications using lignocellulosic feedstocks. It was most recently renamed *Acetivibrio thermocellus* (Tindall, 2019) and prior to that, was renamed *Hungateiclostridium thermocellum* (Zhang et al., 2018) and *Ruminiclostridium thermocellum* (Yutin & Galperin, 2013). However, its longstanding name, *Clostridium thermocellum*, will be used throughout the text for simplicity since it is still the preferred name in the most current literature to date (Wang et al., 2022). *C. thermocellum* is an anaerobic, thermophilic, rod-shaped, spore-forming, Gram-positive bacterium with a lateral flagellum (McBee, 1954). It is capable of degrading cellulose and hemicellulose at a fast rate, and producing a wide range of fermentative end-products (Demain, et al., 2005; Akinosho et al., 2014). The high optimum growth temperature (60-65 ^{o}C) is ideal for CBP production of ethanol as it increases the solubility and digestibility of lignocellulose, reduces contamination

issues, and facilitates product recovery (Demain et al., 2005; Blumer-Schuette et al., 2014). Due to its anaerobic nature, the operational cost to provide adequate oxygen transfer (e.g. for cellulase production in *S. cerevisiae*) during large-scale production is avoided, and more substrate can be converted to end-products instead of cell yield (Demain et al., 2005). Through further development of tools required for genetic manipulation (Biswas et al., 2015; Mazzoli et al., 2020) and metabolic pathway studies (Rydzak et al., 2012), industrial-scale production of various chemicals using *C. thermocellum* may be possible (Akinosho et al., 2014).

1.3.2 Cellulose adherence and utilization

The most distinguishing feature of *C. thermocellum* is its remarkable enzymatic hydrolysis efficiency accomplished by its elaborate cellulosome complex and complementary free enzyme system (Lu et al., 2006; Vazana et al., 2010). The cellulosome is a multiprotein complex that facilitates adhesion of cells to solid substrates and efficient hydrolysis (Bayer et al., 1983; Lu et al., 2006). Deconstruction of lignocellulosic biomass involves a range of enzymatic activities, including cellulases, hemicellulases, xylanases, pectinases, and chitinase (Zverlov et al., 2005). Even though it possesses the ability to deconstruct lignocellulose, *C. thermocellum* does not metabolize the hemicellulose fraction (e.g. xylose, arabinose, mannose, and galactose), which limits the amount of biomass-derived sugars that can be transformed into valuable chemicals (Demain et al., 2005). However, *C. thermocellum* has been deemed to evolve as a cellulose-using "specialist" and ferments the resulting hexose sugars (Lynd et al., 2002).

The cellulosome is a highly efficient, cell-surface enzymatic system that was first discovered in *C. thermocellum* (Bayer et al., 1983). Other bacteria, such as *A. clariflavus* (Izquierdo et al., 2012), *A. cellulolyticus* (Dassa et al., 2012), and *Ruminococcus flavefaciens* (Rincon et al., 2010), also possess cellulosomes but by far, the cellulosome of *C. thermocellum* is

the most well-characterized (Lamed et al., 1983; Hirano et al., 2016). It facilitates close proximity between the bacterium and the substrate, which results in efficient substrate hydrolysis due to the high concentration of cellulolytic enzymes, and immediate uptake of hydrolysis products (Hirano et al., 2016; Lu et al., 2006). Dumitrache *et al*. (2013) demonstrated that *C. thermocellum* forms a monolayer biofilm on the surface of the cellulosic substrate, and suggested that substrate hydrolysis predominantly occurs in this biofilm. *C. thermocellum* biofilms are distinctive as they lack an extracellular polymeric matrix, typically found in biofilms, and cells appear to lay with an orientation parallel to that of the carbon fibres. As biofilm density increased, the cells formed longer chains and began to also lay perpendicular relative to the axis of the carbon fibres, and numerous terminal endospores were observed (Dumitrache et al., 2013). The unique structure and function of *C. thermocellum* biofilms, and the mechanism of cellulose hydrolysis is believed to be an evolutionary strategy embodied by the bacterium (Zhang & Lynd, 2005; Dumitrache et al., 2013).

C. thermocellum is believed to have evolved to function as a cellulose-using "specialist" and exhibits one of the highest growth rates on cellulose (Lynd et al., 2002). Its maximum specific growth rate on model crystalline cellulose substrates in batch culture has been reported from 0.1 h^{-1} on Avicel (Lynd et al., 1989) to 0.16 h^{-1} on α-cellulose (Islam et al., 2009). Cellulose utilization by anaerobic microorganisms is energetically challenging due to the limited ATP available to support both microbial growth and cellulase production (Lynd et al., 2002). This could have led anaerobic microorganisms, like *C. thermocellum*, to develop more efficient mechanisms for cellulose utilization and substrate assimilation. The resulting cellodextrins from cellulose hydrolysis are transported into the cell via an adenosine-binding cassette system with a very high affinity in *C. thermocellum* (Ng & Zeikus, 1982; Strobel et al., 1995). Zhang & Lynd (2005)

concluded that *C. thermocellum* hydrolyzes cellulose into cellodextrins with an average degree of polymerization of at least n = ~4. Assimilating cellodextrins with length ~4 avoids the high ATP requirement for substrate transport through an ABC-type transporter that is typical for anaerobes, while taking advantage of phosphoactivation of each monomer thanks to phosphorolytic cleavage of β-glucan bonds inside the cells (Zhang & Lynd, 2005). The combination of efficient transport and phosphorolytic cleavage of cellodextrins when *C. thermocellum* is grown on cellulose results in sufficient ATP to compensate for the ATP expended for cellulase synthesis (Zhang & Lynd, 2005).

1.3.3 Atypical central metabolism

Conservation of chemical energy, generally in the form of ATP, is common to all organisms in order to support cell growth (Thauer et al., 1977; Marayuma, 1991). During glycolysis, hexose sugars are utilized to produce pyruvate, and electrons are transferred to electron carriers, typically nicotinamide (Taillefer & Sparling, 2016). In aerobic organisms, pyruvate is oxidized completely to produce CO_2, NADH and FADH via the tricarboxylic acid (TCA) cycle. Molecular oxygen is then used to oxidize the reduced electron carriers, resulting in ATP production. Alternatively, anaerobic organisms convert pyruvate and reduced electron carriers into various end products, and ATP is generated through substrate-level phosphorylation (Thauer et al., 1977). The pentose phosphate pathway (PPP) is also available to utilize both hexoses and pentoses to generate NADPH and biosynthetic precursors (Taillefer & Sparling, 2016). The central metabolic pathways of *C. thermocellum* consist of atypical features and are not as well-understood as model microorganisms, such as *E. coli* and *S. cerevisiae* (Zhou et al., 2013). Fermentative end-products, such as ethanol, are direct products of central metabolism, and a more detailed understanding of the various metabolic pathways is important for the exploitation of *C.*

thermocellum and the wide range of fermentative microorganisms with similar industrial potential (Taillefer & Sparling, 2016).

The Embden-Meyerhof-Parnas (EMP) pathway is employed by anaerobic bacteria, including *C. thermocellum*, to oxidize hexose sugars into pyruvate and NADH (Taillefer & Sparling, 2016). The EMP pathway in *C. thermocellum* varies from the canonical EMP pathway as it utilizes different co-factors and lacks a pyruvate kinase, as shown in Figure 1. It has a glucokinase that uses both ATP and GTP, although cell-free extracts displayed higher activity for GTP compared to ATP as a phosphate group donor (Zhou et al., 2013). The genome of *C. thermocellum* contains three putative phosphofructokinases (PFK), one of which was predicted to be PPi-dependent and the remaining two to be ATP-dependent (Rydzak et al., 2012). However, much greater levels of the PPi-dependent PFK expression were observed compared to the others (Rydzak et al., 2012). This was further confirmed by cell-free extracts displaying only PPi-linked activity (Zhou et al., 2013). Its phosphoglycerate kinase displayed approximately equal activity in cell-free extracts with ADP and GDP as cofactors (Zhou et al., 2013).

Genomic analysis revealed *C. thermocellum* does not have any annotated pyruvate kinase genes (Roberts et al., 2010), and this was supported by the lack of pyruvate kinase activity in cell-free extracts (Zhou et al., 2013). However, alternative means for pyruvate generation are present in the genome of *C. thermocellum* including PEP synthase, pyruvate phosphate dikinase (PPDK), PEP carboxykinase (PEPCK), oxaloacetate decarboxylase (OAADC), or a malate shunt pathway (Rydzak et al., 2012). PEP synthase and PPDK can both convert PEP to pyruvate but only PPDK is present at high levels in the proteome (Rydzak et al., 2012) and no PEP synthase activity is observed in cell-free extracts (Zhou et al., 2013). PEPCK, which converts PEP to oxaloacetate, is highly expressed in the proteome (Rydzak et al., 2012) and cell-free extract activity is greater with

GDP than ADP as a cofactor (Zhou et al., 2013). Oxaloacetate can be converted either directly to pyruvate via OAADC, which is highly expressed in the proteome (Rydzak et al., 2012) but no activity has been observed (Taillefer et al., 2015), or go through the malate shunt pathway. It has been suggested that the most likely route for pyruvate generation in *C. thermocellum* is the malate shunt pathway due to high expression levels of malate dehydrogenase and malic enzyme in the proteome (Rydzak et al., 2012). This was further supported by observed cell-free extract activities (Zhou et al., 2013), enzyme purification and characterization (Taillefer et al., 2015), and lethal gene knockouts (Olson et al., 2017). In the malate shunt, a transhydrogenation reaction occurs forming NADPH via oxidation of NADH, which might be utilized in place of the incomplete pentose phosphate pathway for generating NADPH required for biosynthetic reactions (Taillefer et al., 2015).

The pentose phosphate pathway (PPP) connects pentose metabolism with the rest of metabolism by interconverting hexoses and pentoses (Taillefer & Sparling, 2016). It is divided into two distinct branches, the oxidative and non-oxidative branches. The oxidative branch generates NADPH using glucose-6-phosphate from the EMP pathway. The non-oxidative branch generates key biosynthetic precursors, ribose-5-phosphate and erythrose-4-phosphate, required for the synthesis of nucleotides and aromatic amino acids, respectively. *C. thermocellum* does not possess genes encoding glucose-6-phosphate dehydrogenase, gluconolactonase, and 6-phosphogluconate dehydrogenase of the oxidative branch, and as well as transaldolase of the non-oxidative branch (Rydzak et al., 2012). It has been suggested that *C. thermocellum* relies on the EMP pathway to produce intermediates, such as fructose-6-phosphate and glyceraldehyde-3-phosphate, and utilize the fructose-1,6-bisphosphate aldolase and PPi-dependent PFK, along with the transketolase to employ a modified PPP (Rydzak et al., 2012; Taillefer & Sparling, 2016), as

shown in Figure 1. This is supported by high levels of the transketolase throughout fermentation (Rydzak et al., 2012) and PPi-PFK conversion of sedoheptulose-7-phosphate to sedoheptulose-1,7-bisphosphate observed in purified enzyme assays (Koendjbiharie et al., 2020). This proposed PPP is also present in *Entamoeba histolytica* and other parasitic protists (Susskind et al., 1982; Mertens et al., 1993), and could help supply the PPi required for *C. thermocellum* growth.

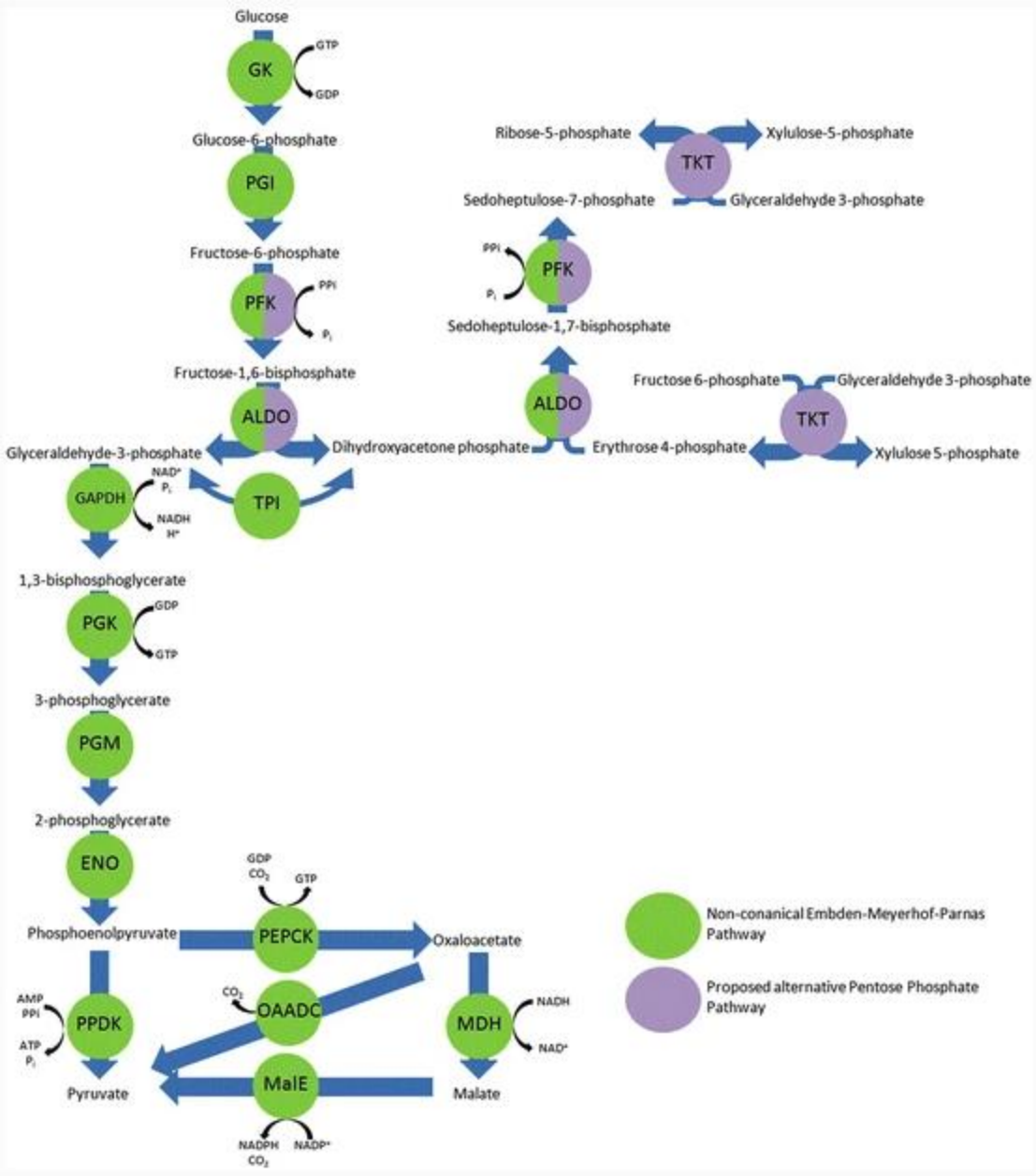

Figure 1. Proposed central metabolic pathways of *C. thermocellum*. GK, glucokinase; PGI, phosphoglucose isomerase; PFK, phosphofructokinase; ALDO, fructose-1,6-bisphosphate aldolase; TPI, triose-phosphate isomerase; GAPDH, glyceraldehyde-3-phosphate dehydrogenase; PGK, phosphoglycerate kinase; PGM, phosphoglycerate mutase; ENO, enolase; PEPCK, phosphoenolpyruvate carboxykinase; MDH, malate dehydrogenase; MalE, malic enzyme; PPDK, pyruvate phosphate dikinase; OAADC, oxaloacetate decarboxylase; TKT, transketolase. This

figure was obtained from Taillefer & Sparling (2016) and reproduced with permission under License Number 5372070112566.

1.3.4 Mixed-product fermentation

Anaerobic microorganisms generate ATP through substrate-level phosphorylation, utilizing organic molecules as electron acceptors (Thauer et al., 1977). This results in reduced electron carriers generated via central metabolism to be oxidized. *C. thermocellum* carries out mixed-product fermentation, as shown in Figure 2 (Rydzak et al., 2009). Its major end-products include H_2, CO_2, formate, acetate, and ethanol, which are produced during the exponential growth of the cells, while minor amounts of lactate are produced as cells enter the stationary phase (Lynd et al., 1989; Sparling et al., 2006). Despite its appealing characteristics, efforts in increasing product yield in *C. thermocellum* for CBP to be industrially viable have only been moderately successful due to its branched fermentation pathways. Bioinformatic analysis of the annotated genome of *C. thermocellum* has identified genes putatively coding for the same annotated function while transcriptomic and proteomic analyses reveal differing expression of these genes under different growth conditions (Carere et al., 2008; Raman et al., 2011; Rydzak et al., 2012).

Pyruvate may be converted into (i) CO_2, reduced Fd, and acetyl-CoA via pyruvate:Fd oxidoreductase (PFOR), (ii) formate and acetyl-CoA via pyruvate:formate lyase (PFL), or (iii) lactate via lactate dehydrogenase (LDH) (Rydzak et al., 2009). Higher CO_2 concentrations compared to formate and lactate produced in batch cultures suggest that the preferential route of carbon flux is through the PFOR (Levin et al., 2006; Rydzak et al., 2012). This is supported by higher expression levels of PFOR compared to PFL and LDH in the proteome (Rydzak et al., 2012). Sparling et al. (2006) detected formate synthesis by *C. thermocellum* grown in cellobiose and α-cellulose, which was confirmed with the detection of transcripts for *pfl* via RT-qPCR and

further supported by detected PFL expression via proteomic analysis (Rydzak et al., 2012). Lactate is a minor end-product of *C. thermocellum*, and LDH expression was detected albeit at low levels compared to PFOR and PFL (Rydzak et al., 2012). However, an increase in lactate production was observed in batch cultures under carbon excess and as cells approached the stationary phase (Islam et al., 2006; Levin et al., 2006). This may be due to the inability of both PFOR and PFL mediated pathways to support the excess carbon flow at the pyruvate branch point, thereby utilizing lactate production as an overflow pathway (Carere et al., 2008).

Further catabolism of acetyl-CoA into ethanol and acetate plays an important role in NADH reoxidation and energy conservation, respectively (Rydzak et al., 2012). The genome of *C. thermocellum* encodes multiple annotated genes for aldehyde dehydrogenase (ALDH) and alcohol dehydrogenase (ADH), which are responsible for ethanol production. It also encodes AdhE, a bifunctional enzyme that can catalyze the reduction of acetyl-CoA to acetaldehyde (ALDH activity) and the reduction of acetaldehyde to ethanol (ADH activity) (Lo et al., 2015). Low expression levels of ALDH suggest that AdhE is predominantly used in ethanol formation (Rydzak et al., 2012). An alternative pathway for ethanol production was demonstrated by Tian et al. (2017). Pyruvate decarboxylase (PDC) from *Acetobacter pasteurianus* (Chandra Raj et al., 2001), which can directly convert pyruvate to acetaldehyde, and ADH from *Thermoanaerobacterium saccharolyticum* (Lo et al., 2015) were expressed heterologously in *C. thermocellum* and resulted in enhanced ethanol formation (Tian et al., 2017). Acetate can be generated from acetyl-CoA directly via acetate thiokinase (ATK) or indirectly via phosphotransacetylase (PTA) and acetate kinase (ACK) (Rydzak et al., 2009). Although both reactions generate ATP, ATK uses AMP and PPi while PTA and ACK uses ADP and Pi (Rydzak, et al., 2009). Acetate production via PTA and ACK is more thermodynamically favourable

compared to using ATK with $\Delta G^{o'}$ = -4 kJ mol^{-1} and +9 kJ mol^{-1}, respectively. However, Raman et al. (2011) reported low mRNA levels of *pta* and *ack*, and higher levels of *atk*, while Rydzak et al. (2012) detected comparable expression levels of all three proteins.

Reduced cofactors generated during central metabolism are oxidized and recycled via H_2 production in *C. thermocellum*. Its genome encodes four putative H_2ases, including an energy conserving (Ech)-like [NiFe]-H_2ase and three Fe-H_2ases (Rydzak et al., 2012). In obligate anaerobic microorganisms, reduced Fd generated from POR-mediated acetyl-CoA generation drives H_2 synthesis via Fd-dependent H_2ases (Charon et al., 1999). Expression levels of the Ech-like Fd-dependent H_2ase in the proteome of wild-type *C. thermocellum* was detected in low amounts or not at all (Rydzak et al., 2012), which is consistent with enzyme activity profiles (Rydzak et al., 2009) and mRNA profiles (Raman et al., 2011). However, proteomic analysis of mutant strains revealed an increase in abundance of some of the Ech-H_2ase subunits though further investigation is required to elucidate the relative importance of this observation (Tian et al., 2016). Reduced Fd could also be oxidized via a bifurcating H_2ase, which utilizes reduced Fd and NADH synergistically in order to overcome the thermodynamic barrier of NADH oxidation to produce H_2 (Schut & Adams, 2009). The two putative NADH-dependent Fe-H_2ases were expressed in high amounts (Rydzak et al., 2012) despite low activities in cell-free extracts (Rydzak et al., 2009), providing a probable method for Fd and NADH reoxidation. The NADPH-dependent Fe-H_2ase has been shown to have 5- to 10-fold higher activity than Fd- and NADH-dependent H_2ases (Rydzak et al., 2006) and is highly expressed in the proteome (Rydzak et al., 2012). This could be a probable method for NADPH re-oxidation to generate H_2 or work in the reverse direction to generate NADPH from H_2 (Calusinska et al., 2010).

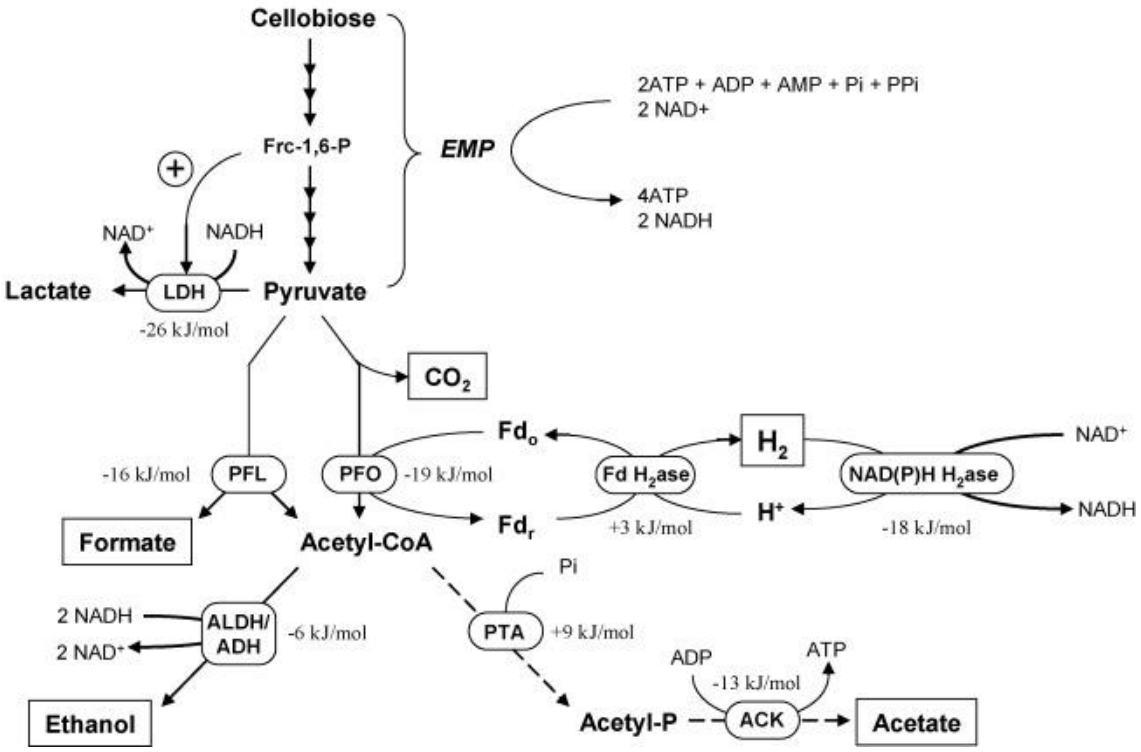

Figure 2. Mixed-product fermentation pathway in *C. thermocellum*. LDH, lactate dehydrogenase; PFL, pyruvate:formate lyase; PFO, pyruvate:Fd oxidoreductase; ALDH/ADH, aldehyde dehydrogenase/alcohol dehydrogenase; PTA, phosphotransacetylase; ACK, acetate kinase. This figure was obtained from Rydzak et al. (2009) and reproduced with permission under License Number 5372070800811.

1.3.5 Overflow metabolism

Carbon availability (Islam et al., 2006; Holwerda et al., 2014) and end-product accumulation (Rydzak et al., 2011; Thompson & Trinh, 2017) have been shown to alter metabolic flux patterns in *C. thermocellum*. In addition to changes in the production of its major fermentation end-products (H_2, CO_2, ethanol, acetate, formate and lactate), secretion of overflow molecules has been reported (Islam et al., 2006; Ellis et al., 2012; Holwerda et al., 2014). Secretion of pyruvate, malate, fumarate, uracil, soluble glucans, amino acids, and an increase in lactate production in *C.*

thermocellum cultures with high initial substrate concentrations are hypothesized to occur due to overflow metabolism (Holwerda et al., 2014). Extracellular pyruvate observed with higher initial cellulose concentrations indicates a metabolic block at the pyruvate branch point due to the rate of carbon catabolism exceeding that of pyruvate consumption (Desvaux et al., 2000). The presence of glycolysis and TCA cycle intermediates, such as malate and fumarate, and soluble glucans in the supernatant is an indication that a metabolic imbalance occurred and the carbon flow was deviated to decrease pyruvate excretion (Zhou et al., 2013; Guedon et al., 2000).

The high rate of carbon catabolism can also result in the flux of carbons and electrons being shifted towards less efficient pathways that produce less or no ATP (Russell & Cook, 1995). Lactate production does not compete with ATP-generating pathways but is a strategy for recycling NADH when the rate of carbon catabolism increases. LDH is regulated by fructose-1,6-bisphosphate (FBP) and an accumulation of FBP due to high rates of carbon flux through glycolysis activates lactate production (Wolin, 1974; Russell & Cook, 1995). Additionally, Ellis et al. (2012) reported that *C. thermocellum* also secretes significant amounts of amino acids, predominantly valine and alanine. Extracellular amino acid concentrations have been found to increase when *C. thermocellum* lactate and acetate production pathways were disrupted (van der Veen et al., 2013), and when cultures were grown at high cellulose loading (Holwerda et al., 2014). Diversion of metabolites from glucose oxidation to amino acid synthesis is bioenergetically costly to cells as it requires the cleavage of high-energy phosphate bonds (Craig & Weber, 1998). However, it may be a strategy utilized to relieve an intracellular redox imbalance by diverting electron flow into the production of alternative reduced end-products, such as amino acids (Holwerda et al., 2014; van der Veen et al., 2013). Reorientation of carbon and electron flows due to substrate concentration has also been observed in other Clostridia species (Szech et al., 1989;

Örlygsson et al., 1995; Desvaux et al., 2000) and demonstrates the high flexibility of the metabolism of these microorganisms.

1.4 Filling in gaps

1.4.1 Natural consortia

In nature, interspecies cross-feeding within complex microbial consortia is important in providing sources of carbon, amino acids, vitamins, and other nutrients to sustain the growth of auxotrophic members (Wolin, 1974; Nozhevnikova et al., 2020). Accumulation of metabolites within a cell or in the environment of the cell may trigger metabolic responses in the absence of other microbial species (Weimer & Zeikus, 1977; Holwerda et al., 2014). One important example of metabolic association between interacting microbial species is interspecies hydrogen transfer, in which electrons from H_2 produced by chemoorganotrophs through fermentation are transferred to methanogens for CH_4 generation (Stams & Plugge, 2009). This association is also beneficial to fermenters as continuous consumption of H_2 by methanogens maintains sufficiently low concentrations of H_2 for fermentation to remain thermodynamically favourable (Thauer et al., 1977; Weimer & Zeikus, 1977). *C. thermocellum* was first isolated from manure (Viljoen et al., 1926) and further strains have been isolated from soil, compost (Ozkan et al., 2001), and anaerobic digesters (Burrell et al., 2004), where highly diverse and complex microbial communities commonly exist (Lynd et al., 2002). Investigation of such interactions could give more insight and is valuable in filling in gaps in our knowledge of the metabolism of *C. thermocellum* and closely-related microorganisms with similar potential.

1.4.2 Targeting H_2 production in *C. thermocellum*

A major obstacle to metabolic engineering of *C. thermocellum* to increase end-product yield is the incomplete knowledge of its complex metabolism. Several studies have suggested that *C. thermocellum* has an atypical central metabolism in which non-canonical co-factors and enzymes are utilized (Zhou et al., 2013; Rydzak et al., 2012; Koendjbiharie et al., 2020). Its branched fermentation pathways produce a wide range of end-products (e.g. ethanol, acetate, H_2, CO_2, formate and lactate) along with amino acids, in some cases (Sparling et al., 2006; Ellis et al., 2012). Numerous mechanisms used by cells to maintain cellular redox employ various enzymes that are, in many cases, redundant and are affected by many factors, including the accumulation of end-products (Carere et al., 2014). Further investigation of carbon and electron flux through *C. thermocellum* fermentation pathways can provide a more detailed understanding of its complex metabolism required to aid in future metabolic engineering efforts to increase end-product yield. In this thesis, we focus on H_2 production in *C. thermocellum* which plays a key role in redox balancing and has been shown to significantly affect metabolic flux distributions (Weimer & Zeikus, 1977; Biswas et al., 2015).

H_2 production is catalyzed by H_2ases using electrons from reducing equivalents (reduced Fd, NADH and NADPH) generated from carbohydrate catabolism (Raman et al., 2011). The H_2ases of *C. thermocellum* have been investigated in several studies to elucidate the H_2 generation pathways in *C. thermocellum* (Carere et al., 2008; Rydzak et al., 2009; Raman et al., 2011; Rydzak et al., 2012). These studies suggest that *C. thermocellum* utilizes bifurcating H_2ases, which use reduced Fd and NADH, and NADPH-dependent H_2ase for H_2 synthesis. The presence of an Ech-like Fd-dependent H_2ase in the genome of *C. thermocellum* suggests that it could employ a membrane-bound Fd-dependent H_2ase for H_2 synthesis, similar to what has been described in

Thermoanaerobacter tengcongensis (Soboh et al., 2004). Ech-like H_2ase and NADH:Fd oxidoreductase can reoxidize reduced Fd and pump H^+/Na^+ ions across the cell membrane, creating a proton gradient for ATP synthesis (Vignais et al., 2001; Raman et al., 2011). However, expression of the Ech-like Fd-dependent H_2ase in *C. thermocellum* was detected at low levels or not at all (Raman et al., 2011; Rydzak et al., 2012). This leads to the question of why an advantageous Ech-like H_2ase is not being expressed in *C. thermocellum*.

H_2ase-mediated oxidation of reducing equivalents becomes thermodynamically unfavourable when localized H_2 concentrations are high, inhibiting H_2 synthesis and shifting carbon flux distribution (Lamed et al., 1988; Levin et al., 2006). Carere et al. (2014) reported that removal of H_2 (and CO_2) via N_2 sparging in batch cultures of *C. thermocellum* changed the end-product profile but did not significantly change enzyme activity and expression of the H_2ases. Only minor differences in generation time and final biomass concentration were observed despite changes in end-products, namely acetate production, which is associated with ATP generation. This study suggested that thermodynamics plays a significant role in the manipulation of carbon and electron fluxes rather than enzyme activity and gene expression in *C. thermocellum*. Although, sparging with N_2 removed H_2 in the headspace while dissolved H_2 (H_{2aq}), which is suggested to be a more appropriate predictor of H_2ase inhibition during fermentation, may not have decreased sufficiently to cause changes in enzyme activity and/or gene expression. Weimer and Zeikus (1977) reported altered growth and end-product patterns with no free H_2 detected in *C. thermocellum* grown in the presence of a methanogen, *Methanobacterium thermoautotrophicum*, on cellulose. In this thesis, we propose that continuously removing H_2, in the headspace and H_{2aq}, during fermentation via consumption by a methanogen in co-culture may reveal other physiological and metabolic changes in *C. thermocellum*. Co-culturing *C. thermocellum* with a

methanogen allows us to investigate *C. thermocellum* in more natural consortium conditions, in which accumulation of fermentation end-products is not permitted due to the presence of a naturally occurring partner.

1.4.3 *Methanothermobacter marburgensis*

Methanothermobacter marburgensis (formerly *Methanobacterium thermoautotrophicum* strain Marburg) is an anaerobic, thermophilic, methanogenic Archaea (Wasserfallen et al., 2000) that was isolated from an anaerobic sewage digester in Marburg, West Germany (Hungate, 1969; Fuchs et al., 1978). It grows optimally at 65 ºC, utilizes H_2/CO_2 as its sole energy source and CO_2 as its sole carbon source, and produces CH_4 as an end-product. It belongs to the order of *Methanobacteriales* along with *Methanothermobacter thermoautotriphicus*, formerly *Methanobacterium thermoautotrophicum* strain ΔH (Wasserfallen et al., 2000). Although *M. marburgensis* and *M. thermoautotrophicus* are closely related, with a 16S rRNA sequence identity of 98.7% (Wasserfallen et al., 2000), the former has a shorter doubling time compared to the latter, $\leq$ 2 hours (h) and 5 h, respectively (Kaster et al., 2011). Methanogens, such as *M. marburgensis*, act as 'electron sinks' for chemoorganotrophs, such as *C. thermocellum*, making it energetically feasible to dispose of electrons as H_2 rather than as other reduced end-products, such as ethanol, lactate, and extracellular amino acids, during fermentation (Weimer & Zeikus, 1977). Growing *M. marburgensis* and *C. thermocellum* in co-culture also offer the possibility to investigate the physiology of *M. marburgensis* in a more natural consortium setting where concentrations of H_2 and CO_2 are lower.

1.5 Research objectives

The objective of this project is to investigate changes in the physiology of *Clostridium thermocellum* when H_2 is continuously removed during fermentation via consumption by *Methanothermobacter marburgensis*. We hypothesized that *C. thermocellum* and *M. marburgensis* are interacting in close proximity when co-cultured during which *M. marburgensis* will act as an 'electron sink' for *C. thermocellum*, resulting in changes in the fermentation and overflow metabolism end-product profile and an increase in transcription of *C. thermocellum* H_2ases. This project specifically aims to:

1. Investigate the effects of co-culturing on the growth and end-product synthesis of *C. thermocellum* and *M. marburgensis*;
2. Determine if *C. thermocellum* and *M. marburgensis* are interacting in co-culture; and
3. Investigate the effect of continuous H_2 removal by *M. marburgensis* in *C. thermocellum* H_2ase gene expression.

Chapter 2: MATERIALS AND METHODS

2.1 Microorganisms and Media

Clostridium thermocellum DSM 1237 and *Methanothermobacter marburgensis* DSM 2133 were obtained from Deutsche Sammlung von Mikroorganismen und Zellkulturen (Braunschweig, Germany). Fresh cultures of *C. thermocellum* were maintained by adding 10% (*v/v*) inoculum into anaerobically prepared minimal nutrient medium (MNM) with 2 g/L Avicel. Fresh cultures of *M. marburgensis* were maintained by adding 10% (*v/v*) inoculum into MNM medium that was prepared anaerobically by gassing with a mixture of 80% H_2 and 20% CO_2, and fed with the same gas mixture every 24 hours (h) for 2-3 days (Kaster et al., 2011). All cultures were incubated at 60°C in an upright position without shaking.

Minimal nutrient media (MNM) was prepared according to Kridelbaugh et al. (2013), with modifications to facilitate *M. marburgensis* growth, and contained 8.3 mM NH_4Cl, 47.8 mM MOPS, 19.8 mM NaCl, 20.4 mM KCl, 6.9 mM K_2HPO_4, 6.4 mM L-cysteine·HCl·H_2O, 4.9 mM $MgCl_2 \cdot 6H_2O$, 1 mM $CaCl_2 \cdot 2H_2O$, 0.2 mg/mL resazurin, 1 mL/L vitamin solution, and 1 mL/L trace mineral solution. Vitamin solution contained the following (per litre): 0.4 mg pyridoxamine·2HCl, 0.2 mg biotin, 0.4 mg PABA, and 0.2 mg vitamin B_{12}. Trace mineral solution (pH 6.7) contained the following (per litre): 0.5 mg $MnCl_2 \cdot 4H_2O$, 0.5 mg $CoCl_2 \cdot 6H_2O$, 0.08 mg $ZnCl_2$, 0.04 mg $CuCl_2 \cdot 2H_2O$, 0.05 mg $Na_2MoO_4 \cdot 2H_2O$, 0.05 mg $NiCl_2 \cdot 6H_2O$, 29.2 mg EDTA (free acid), and 1 mg $FeCl_2 \cdot 4H_2O$. Media for *C. thermocellum* in the presence and absence of *M. marburgensis* were adjusted to pH 7.0 to 7.2 with 5 M NaOH, and underwent four cycles of 1 min vacuum followed by 1 min gassing with N_2. Media for *M. marburgensis* were adjusted to pH 8.8-9.0 with 5 M NaOH, and underwent four cycles of 1 min vacuum followed by 1 min gassing with an 80:20 mixture of H_2 and CO_2, respectively, leading to an in situ pH of 6.8 to 7.2. All culture

media were autoclaved for 30 min at 121°C. All reagent-grade chemicals were purchased from Sigma-Aldrich Co. and compressed gases were purchased from Welder's Supply (Manitoba, Canada).

2.2 Experimental Design

All experiments were performed in serum bottles (120 mL, Wheaton) sealed with butyl rubber stoppers and aluminum crimp caps (Supelco brand, Sigma-Aldrich). Avicel PH-101 was obtained from Sigma-Aldrich and unmercerized cotton was obtained from Lunatic Fringe Yarns (Idaho, USA). Substrates were added to the medium during its preparation. Final concentrations of Avicel were 2 g/L for growth, end-product and gene expression analyses, and 10 g/L for analyses of additional secreted end-products under high carbon loading. Cotton was used as a carbon source by *C. thermocellum* and a substrate for the cells to bind to while growing in liquid culture for scanning electron microscopy examination. Cotton was cut in 5 cm length (equivalent to 0.02 g in weight) and added to 9 mL MNM medium. Since *M. marburgensis* does not hydrolyze or utilize cellulose, it was grown in media that was gassed with 80% H_2 and 20% CO_2, which allows for comparison of *M. marburgensis* growth under high- and limiting-concentrations of H_2 and CO_2. Experimental cultures were prepared by inoculating 5% (*v/v*) of stationary phase *C. thermocellum* (10^8 genomes/mL) and 10% (*v/v*) exponential phase *M. marburgensis* (10^9 genomes/mL). Volume differences between monocultures and co-cultures were corrected via addition of sterile, anaerobic MNM medium. All cultures were incubated at 60°C in an upright position without shaking.

2.3 End-product Analyses

Gaseous end-products (H_2, CO_2, and CH_4) in the headspace were measured by thermal conductivity with a Varian micro-GC (Agilent), using nitrogen as the carrier gas. Headspace

sampling was performed using a 3 mL syringe. Concentrations of H_2, CO_2, and CH_4 were calculated from headspace measurements, and gas solubility using Henry's law and equilibrium dissociation constants (Sander, 2015). Concentrations of samples were determined by comparison to linear standard curves of each gas. The amount of dissolved CO_2 was calculated using the sample's pH and using the Henderson-Hasselback equation. Major liquid end-products and soluble sugars were measured using a high-performance liquid chromatography (HPLC) system (Waters) with an HPX-87H column (Bio-Rad) and a refractive index detector (Waters). Culture supernatants were acidified with 5 mM H_2SO_4 at a 1:1 ratio. Samples were run at a flow rate of 0.6 mL/min with 5 mM H_2SO_4 as the mobile phase, at a temperature of 45 ^oC. A dilution series of cellobiose, glucose, pyruvate, lactate, formate, acetate, and ethanol were prepared with 5 mM H_2SO_4 to construct linear standard curves for concentration measurements in samples.

2.4 GC-MS Analysis for Additional End-products

The gas chromatography-mass spectrometry (GC-MS) analysis and data collection were performed by the Goodman Cancer Research Centre Metabolomics Core Facility (McGill University, Canada) for relative quantification of alternate end-products of *C. thermocellum* and *M. marburgensis*. Aliquots of supernatants (50 µl) were transferred to sample tubes and kept on ice. 500 µl of cold 80% methanol was added to each sample tube, vortexed briefly, and centrifuged at 15,000 rpm for 10 minutes at 4 ^oC. The resulting supernatants were added to new sample tubes containing 1 µl of 800 ng/µl Myristic-d27 in pyridine (internal standard) and dried in a CentriVap Concentrator at -4^oC overnight (Faubert et al., 2013). The samples were prepared for GC-MS analysis by adding 30 µl of MOX (10 mg Methoxyamine:HCl per 1 mL anhydrous pyridine) to each sample and incubating at room temperature for 30 minutes. The samples were derivatized

with 70 µl of MTBSTFA for 30 minutes at 70ºC to form more volatile TBDMS derivatives. Data acquisition was done in Scan and SIM modes.

Standards for generation of calibration curves were prepared by serially diluting LC-MS standards in water, followed by drying in a CentriVap concentrator at -4 ºC. The standards were methoximated and derivatized for GC-MS analysis in the same manner as the supernatant samples. LC-MS standards include the following: amino acids (excluding arginine and ornithine), TCA cycle intermediates (including citrate, cis-aconitate, isocitrate, 2-ketoglutarate, succinate, fumarate, malate, oxaloacetate), glycolysis intermediates (including dihydroxyacetone-phosphate, glyceraldehyde-3-phosphate, 3-phosophoglycerate, 2-phosphoglycerate, phosphoenolpyruvate, pyruvate), lactate, glycolic acid, sarcosine, urea, glyceraldehyde, uracil, adenine, taurine, hypotaurine, phosphoric acid, 4-morpholineethanesulfonic acid, 2-hydroxyglutarate, and hypoxanthine. Only metabolites with calibration samples and good peak shapes were reported in this thesis.

2.5 Residual cellulose

Residual cellulose in samples was measured by quantitative saccharification, following Kridelbaugh et al. (2013) with some modifications. Cultures were mixed to resuspend residual cellulose and 1 mL of sample was taken, followed by centrifugation at 14 000 x g for 2 mins in a Sorvall Legend Micro 21 R centrifuge. The resulting pellet was washed with 0.9% NaCl and resuspended in 50 µl of 72% (w/w) H_2SO_4. The mixture was incubated at 30 ºC for 1 hour. The acid was diluted to 4% (w/w) by the addition of 850 µl of water and autoclaved for 20 mins at 121ºC. The hydrolyzed samples were analyzed by HPLC (see Section 2.3 End-product Analyses). A dilution series of hydrolyzed cellulose and glucose was prepared to construct linear standard curves for calculating concentrations of samples.

2.6 DNA extraction and qPCR

Cultures grown on Avicel were mixed to resuspend cells and 1 mL of sample was taken, followed by centrifugation at 14 000 x g for 2 mins in a Sorvall Legend Micro 21 R centrifuge. Biofilm cells on cotton were enumerated by carefully isolating the cotton from the fermentation broth while planktonic cells were enumerated by taking 1 mL of liquid culture to obtain the cell pellet. The cotton and resulting pellet were used for DNA extraction with InstaGene Matrix (Bio-Rad), following the manufacturer's protocol. qPCR was performed with fluorescent probes designed to target the *cpn60* gene in *C. thermocellum* (5'-FAM/3'-Blackhole quencher) and *radA* gene in *M. marburgensis* (5'-HEX/3'-Blackhole quencher) (Nadkarni et al., 2002; Hill et al., 2005). PCR primers and probes were designed using the NCBI primer designing tool (https://www.ncbi.nlm.nih.gov/tools/primer-blast/). Target genes and their corresponding primer and probe sequences are shown in Table 1. qPCR reactions were performed in triplicate and contained (20 µl total volume per reaction): 10 µl of iQ Multiplex Powermix, 2 x 0.6 µl of 25 µM forward and reverse primers, 0.4 µl of probe, 2 µl of template DNA, and dH_2O to 20 µl. Thermo-cycling was performed in a CFX Connect Real-Time System (Bio-Rad) and cycling conditions were: 95°C for 3 min, and 40 cycles of 95°C for 10s, 56°C for 10s, and 72°C for 30s. Standard curves for each species were prepared by extracting DNA from concentrated cells, calculating the number of genome copies, based on total DNA concentration and size of genomes, and creating a serial dilution series of the extracted DNA. Total DNA concentration was measured using a NanoDrop (Thermo Fisher Scientific). PCR efficiencies calculated from generated standard curves are between 90% and 110%.

Table 1. Primer and probe sequences used for cell enumeration.

Primer/ probe	Sequence (5'→ 3')	Target (locus tag)	Amplicon length (bp)
CT-F	TCCTCATTACAGACAAGAA	*Clostridium thermocellum cpn60* (Cthe_2892)	147
CT-R	CCTCTTAATTTGTTTACAAGC		
CT-probe[1]	CCTCAACATCCTCAGCAATGATAACC		
MM-F	GCTATCCCATGAACTAGCAG	*Methanothermobacter marburgensis radA* (MTBMA_c17700)	114
MM-R	CTGCTCTATCCTTTCAGGAC		
MM-probe[2]	GGGGTGGCCTGGATGCTGAGGC		

[1]5'-FAM, 3'-Blackhole quencher

[2]5'-HEX, 3'-Blackhole quencher

2.7 Scanning Electron Microscopy

Each cotton strand was carefully isolated from the liquid culture and fixed in modified Karnovsky's fixative (2.5% glutaraldehyde, 1% paraformaldehyde, 0.1 M phosphate buffer, pH 7.2-7.4) at 4°C for 2 hours. The samples were washed with 0.1 M phosphate buffer and incubated with 1% osmium tetroxide (Cedarlane) in 0.1 M phosphate buffer for 1 hour. Fixed samples were washed with 0.1 M phosphate buffer followed by dehydration through serial transfers in ethanol concentrations of 70%, 80%, 95%, and 100% (anhydrous). Samples were transferred in hexamethyldisilazane (Cedarlane) (Laforsch & Tollrian, 2000), which was left to completely evaporate in the fume hood. Samples were visualized on a Hitachi TM 1000 tabletop SEM equipped with a backscatter detector.

2.8 RNA Extraction and RT-qPCR

Samples (50 mL) of exponential phase *C. thermocellum* grown in the presence and absence of *M. marburgensis* on 2 g/L Avicel were processed immediately following harvest by centrifugation in a Sorvall RC6 centrifuge with an SH-3000 rotor at 4 500 x g for 10 minutes and resuspended in 5-10 volumes of RNA*later* solution (Invitrogen). Samples were stored at -20°C in RNA*later* until all cultures were ready. Total RNA was isolated using TRIzol reagent (Invitrogen) according to the manufacturer's instructions for cells grown in suspension, with some modifications to improve RNA yield and purity (Toni et al., 2018). An additional bead-beating step was included for efficient Gram-positive cell lysis. 1 mL aliquots of cells suspended in TRIzol reagent were transferred to 2 mL screw-cap tubes that contain lysis beads and cell lysis proceeded with 6 cycles of 30 sec bead beating treatments at 2.75 m sec^{-1} in a Bead Mill Homogenizer (OMNI International). Cell lysates were centrifuged at 12 000 x g for 10 mins at 4°C to remove insoluble material and supernatant was transferred to fresh Eppendorf tubes. A second chloroform extraction step was done to remove excess phenol and protein contamination. RNA pellets were washed 3 times with 75% ethanol to remove residual salts and dissolved in DEPC-treated RNase-free water (Invitrogen). RNA preparations were treated with DNase I (0.1 U/µL) (Thermo Fisher Scientific) in a reaction buffer with $MgCl_2$ for 30 mins at 37°C to remove genomic DNA. The treated RNA was re-purified using the GeneJET RNA purification kit (Thermo Fisher Scientific), according to the manufacturer's protocol for RNA cleanup.

cDNA synthesis was accomplished with SuperScript VILO cDNA synthesis kit (Invitrogen), following the manufacturer's recommended protocol. Reaction mixtures containing RNA (up to 2.5 µg), 1X VILO reaction mix, 1X SuperScript Enzyme mix, and DEPC-treated water

were incubated in a T100 thermal cycler (Bio-Rad) with the following cycling conditions: 25°C for 10 mins, 42°C for 60 mins, and 85°C for 5 mins.

Hydrogenase (H_2ase) primers were designed by Carere et al. 2014, and correspond to the three [FeFe] (Cthe_0430, Cthe_3003, and Cthe_0342) and one [NiFe] (Cthe_3020) H_2ase catalytic subunits of *C. thermocellum*. Values were normalized to the *recA* gene (Cthe_1050), which encodes a DNA recombination protein in *C. thermocellum*. Primers were designed using the NCBI primer designing tool (https://www.ncbi.nlm.nih.gov/tools/primer-blast/). All primer nucleotide sequences used for RT-qPCR are listed in Table 2. qPCR reactions were performed in triplicate and contained 1X FAST SYBR Green Master Mix (Applied Biosystems), forward and reverse primers (200 nM each), DEPC-treated water, and synthesized cDNA (20 ng). Reactions were run in a CFX Connect Real-Time System (Bio-Rad) with the following cycling conditions: 95°C for 20 sec, and 40 cycles of 95°C for 3 sec and 60°C for 30 sec. PCR efficiencies from generated standard curves of extracted *C. thermocellum* DNA are between 90% and 110%.

Table 2. Primer sequences used for comparative quantification of H_2ase expression.

Locus tag	Annotation	Forward (5'→ 3')	Reverse (5'→ 3')
Cthe_3020	[NiFe] H_2ase	GCCAGTGCATATCCCTCATT	GGTTGGAGTACGAACCCTGA
Cthe_0342	[FeFe] H_2ase	AGGAGCCGTCTGAACGACTA	TGTGTCAGCATGTGCAAGAA
Cthe_3003	[FeFe] H_2ase	CCGGAATACTGTTTGGTGCT	TCTTAAGGCCGCTGACAACT
Cthe_0430	[FeFe] H_2ase	AGGAGCCGGTGTGATATTTG	CGCTGACCACTGCAACTTTA
Cthe_1050	RecA	TTGTTTCCCAGCCGGATACC	TGGGACATAAGCCTTGCCTG

2.9 Data analysis

The standard curves for liquid end-products and sugars were prepared using triplicate data points from a dilution series run at the same time samples were in the HPLC. Three technical replicates of headspace gas measurements were taken and the mean was used to calculate the concentration of the sample. Gas measurements were used to track the growth of *C. thermocellum* and *M. marburgensis* for sampling when grown on cotton, high carbon, and for gene expression. Carbon balance and oxidation/reduction (O/R) index (Eq. 1 and Eq. 2, respectively) were calculated from end-product measurements to compare the distribution of carbon and electrons in *C. thermocellum* in monoculture and *C. thermocellum* in co-culture with *M. marburgensis*. All PCR primers were checked for cross-reactivity prior to use.

([lactate]/2 + ([acetate] + [ethanol])/3 + ([CO_2] + [formate])/6) ÷ [cellulose utilized (as mM glucose equivalent)] Equation 1

$(2*[CO_2] + [formate]) \div (2*[ethanol] + [H_2])$ Equation 2

C. thermocellum primers (cpn60, recA and H_2ases) did not react with *M. marburgensis* extracted DNA and *M. marburgensis* radA primers did not react with *C. thermocellum* extracted DNA. Relative expression of genes was calculated using the $2^{-\Delta\Delta Ct}$ method with *C. thermocellum* grown in the absence of *M. marburgensis* as the calibrator (Livak & Schmittgen, 2001). All statistical analyses, unless otherwise indicated, were performed using Microsoft Excel. The statistical significance of expression ratios was determined using the BootstRatio web application (http://regstattools.net/br) (Clèries et al., 2012) with the setting for data that have been already normalized against a control sample, *C. thermocellum* grown in monoculture. While the data presented in Chapter 3 are results from one data set, experiments and analyses were repeated and the data presented are representative of the results from the repeated experiments/analyses.

Chapter 3: RESULTS

3.1 Growth parameters

To determine the effect of growing *C. thermocellum* in co-culture with *M. marburgensis*, monocultures of each species were also grown in MNM with 2 g/L cellulose over 40 hours and samples were taken every 4 hours for analyses. The cell concentration profiles of *C. thermocellum* and *M. marburgensis* over the course of fermentation, based on qPCR measurements of genomic copies of *cpn60* (for *C. thermocellum*) and *radA* (for *M. marburgensis*), are shown in Figure 3. *C. thermocellum* grown in monoculture exhibited a longer lag period than *C. thermocellum* grown in co-culture with *M. marburgensis*, 12 h and 8 h, respectively. *M. marburgensis* grown in co-culture with *C. thermocellum* exhibited a 12 h lag period while no lag period was observed in *M. marburgensis* grown in monoculture. A more intense yellow coloration (Ait et al., 1982) was observed on the cellulose in co-cultures earlier than in *C. thermocellum* monocultures and no colour (Wasserfallen et al., 2000) was observed on the cellulose in *M. marburgensis* monocultures. The growth rate and maximum cell concentration of *C. thermocellum* in co-cultures (0.39 h^{-1} and 1.32 x 10^{10} genomes/mL, respectively) did not change significantly from that of *C. thermocellum* in monocultures (0.49 h^{-1} and 1.94 x 10^{10} genomes/mL, respectively). In contrast, *M. marburgensis* in monocultures (4.6 x 10^{11} genomes/mL) grew significantly more than *M. marburgensis* in co-cultures (1.85 x 10^{10} genomes/mL), with cell concentrations increasing 90-fold in monocultures and up to 4-fold in co-cultures. A thin white layer, presumably of *M. marburgensis* cells (Wasserfallen et al., 2000), was also observed on the liquid-gas interphase in the *M. marburgensis* monoculture. *M. marburgensis* growth and methanogenesis were limited by the rate of H_2 and CO_2 production by *C. thermocellum* in the co-cultures.

Detectable cellulose hydrolysis was observed at 12 hours post-inoculation (h pi) for both *C. thermocellum* cultures but *C. thermocellum* in co-cultures hydrolyzed cellulose at a faster rate than *C. thermocellum* in monocultures (Figure 4A). At 16 h pi, *C. thermocellum* in co-cultures appears to have hydrolyzed 30% of the cellulose while *C. thermocellum* in monocultures hydrolyzed only 10% of the cellulose. During stationary phase, there was still 1.1 g/L and 0.8 g/L of residual cellulose in *C. thermocellum* monocultures and co-cultures, respectively, despite growth of cells ceasing. Complete cellulose hydrolysis was achieved faster by *C. thermocellum* in co-cultures with *M. marburgensis*. pH in co-cultures decreased earlier compared to *C. thermocellum* in monocultures, but culture pH was similar upon entry into the stationary phase, 6.8, and both reached a minimum pH of 6.7 (Figure 4B).

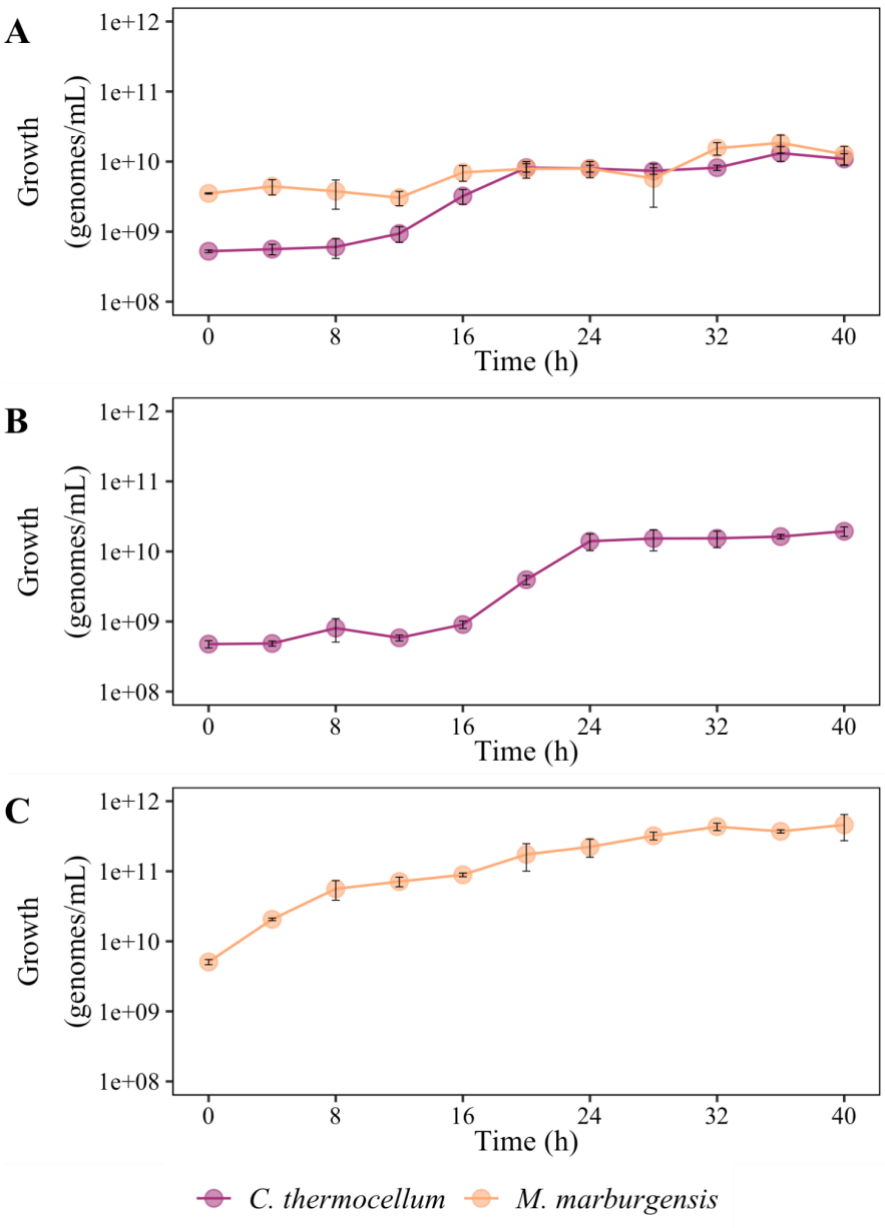

Figure 3. Growth of *C. thermocellum* and *M. marburgensis* in co-culture (A), *C. thermocellum* in monoculture (B), and *M. marburgensis* in monoculture (C). *C. thermocellum* in co-culture and monoculture were grown with 2 g/L cellulose while *M. marburgensis* in monoculture were grown with 80% H_2 and 20% CO_2. Each data point represents the mean of three biological replicates and error bars denote the standard deviations.

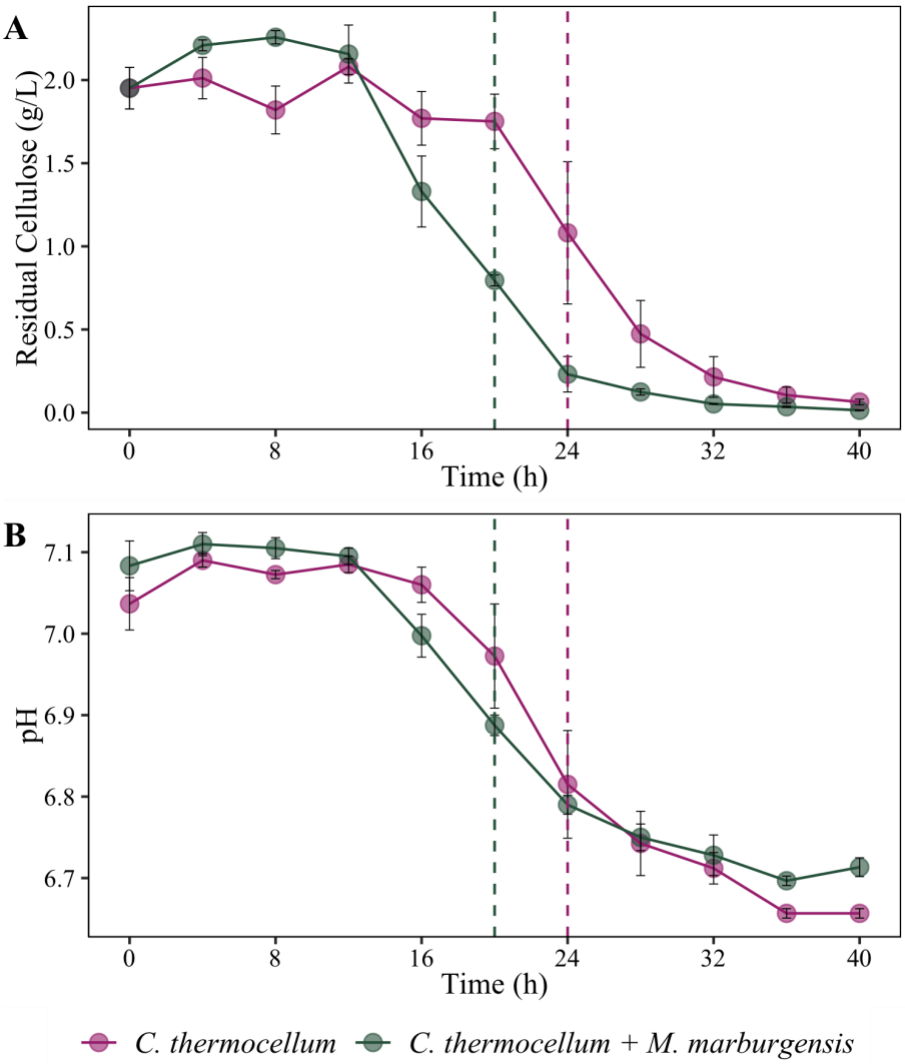

Figure 4. Cellulose hydrolysis (A) and pH (B) in *C. thermocellum* monoculture and *C. thermocellum* and *M. marburgensis* co-culture when grown with 2 g/L cellulose. Dashed lines show when the stationary phase started for each culture condition. Each data point represents the mean of three biological replicates and error bars denote the standard deviations.

3.2 Fermentation end-products

The end-product profile of *C. thermocellum* grown in monocultures and in co-cultures with *M. marburgensis* were compared over the course of fermentation (Figure 5 and 6). Table 3 shows a comparison of the final end-product concentrations, carbon balance and O/R index in *C. thermocellum* monocultures and *C. thermocellum* and *M. marburgensis* co-cultures. H_2, CO_2, acetate, and ethanol were the major detected end-products with formate and lactate produced in minor amounts by *C. thermocellum* grown in monocultures with 2 g/L cellulose, as shown in Figure 5B and Figure 6B. The production of H_2, CO_2, acetate, ethanol, and formate began early in the exponential phase and continued in the stationary phase. Lactate was produced late in the fermentation after production of most other end-products had ceased. The major end-products detected in *C. thermocellum* and *M. marburgensis* co-cultures grown with 2 g/L cellulose are CO_2, acetate, and ethanol, as shown in Figure 5A and Figure 6A. Acetate concentration increased over 1.5 times in co-culture relative to *C. thermocellum* in monoculture and production continued during the stationary phase. Formate and ethanol production decreased and ceased during late exponential to early stationary phase. No significant change in lactate production was observed in the co-cultures compared to the *C. thermocellum* monoculture. H_2 levels remained low throughout the course of fermentation, with the minimum detected concentration being 0 mM and the maximum detected concentration being 1.2 mM.

The concentration of H_2 and CO_2 produced by *C. thermocellum* in co-cultures can be estimated using the detected concentrations of H_2, CO_2 and CH_4, as shown in Figure 5C. In co-culture with *M. marburgensis*, it was calculated that *C. thermocellum* produced up to 21.4 mM of H_2 and 15.3 mM of CO_2, both ~20% higher than what was produced in monoculture, based on the assumption that one mole of CH_4 is formed by the oxidation of four moles of H_2 and the reduction

of one mole of CO_2. Although significantly less H_2 was detected due to continuous consumption by *M. marburgenis*, H_2 remains a major end-product of *C. thermocellum* in the co-culture. The carbon balance and O/R index were calculated using the detected end-product concentrations in *C. thermocellum* monocultures, and the detected and calculated end-product concentrations in *C. thermocellum* and *M. marburgensis* co-cultures at the end of fermentation (40 h pi), as shown in Table 3. The carbon balance is 0.70 in the *C. thermocellum* monoculture and 0.85 in the *C. thermocellum* and *M. marburgensis* co-culture, which indicates that there is missing carbon that was not accounted for. All electrons were accounted for in *C. thermocellum* grown in monoculture (1.0) while the O/R index increased in the *C. thermocellum* and *M. marburgensis* co-culture (1.2), indicating that there are more oxidized end-products compared to reduced end-products.

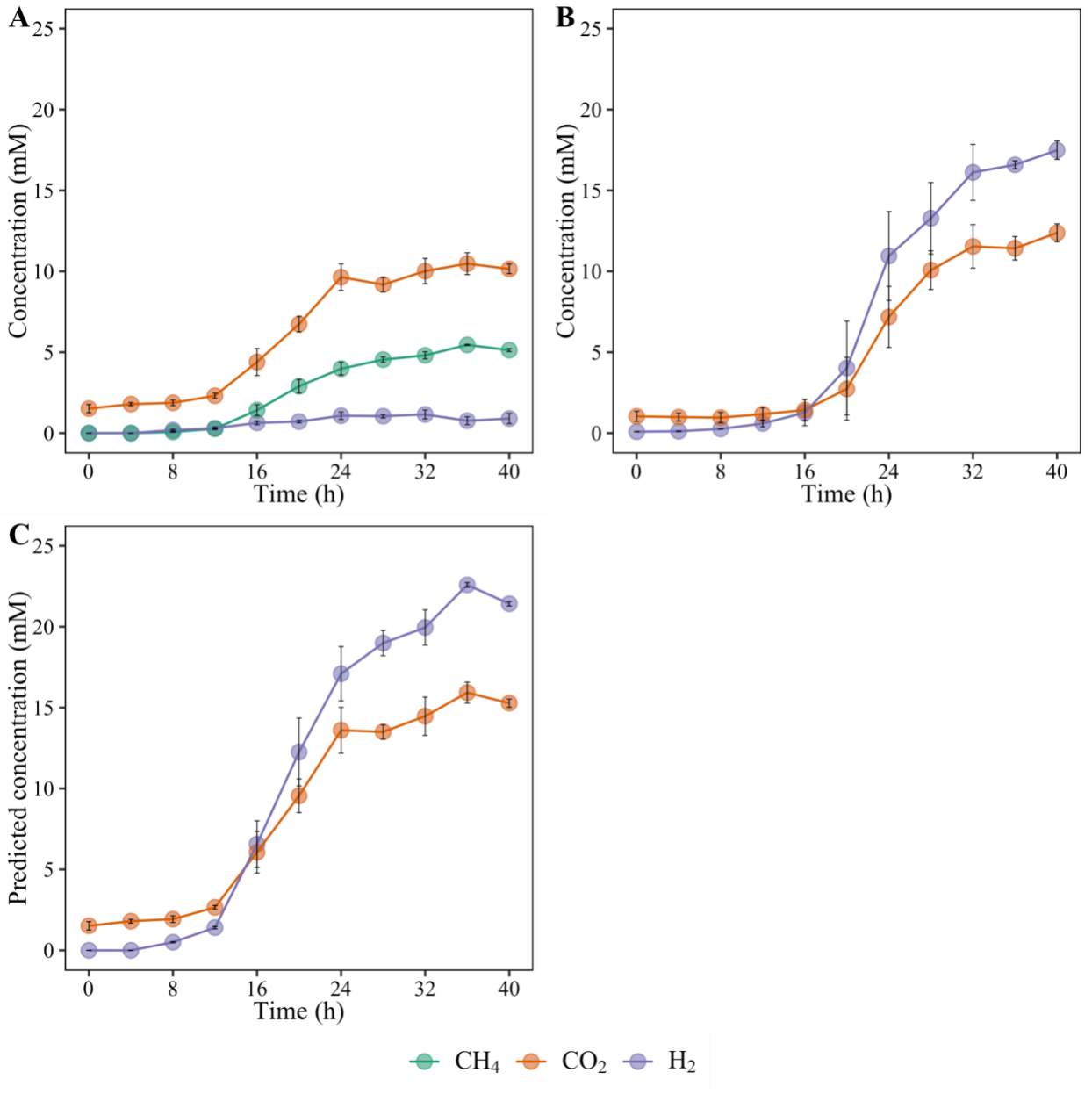

Figure 5. Detected concentrations of gases produced by *C. thermocellum* and *M. marburgensis* co-culture (A) and *C. thermocellum* monoculture (B), and calculated concentrations of gases produced by *C. thermocellum* in co-culture with *M. marburgensis* (C) when grown with 2 g/L cellulose. Calculated concentrations of H_2 and CO_2 produced by *C. thermocellum* in co-culture with *M. marburgensis* were based on CH_4 concentrations in Figure 5A. Each data point represents the mean of three biological replicates and error bars denote the standard deviations.

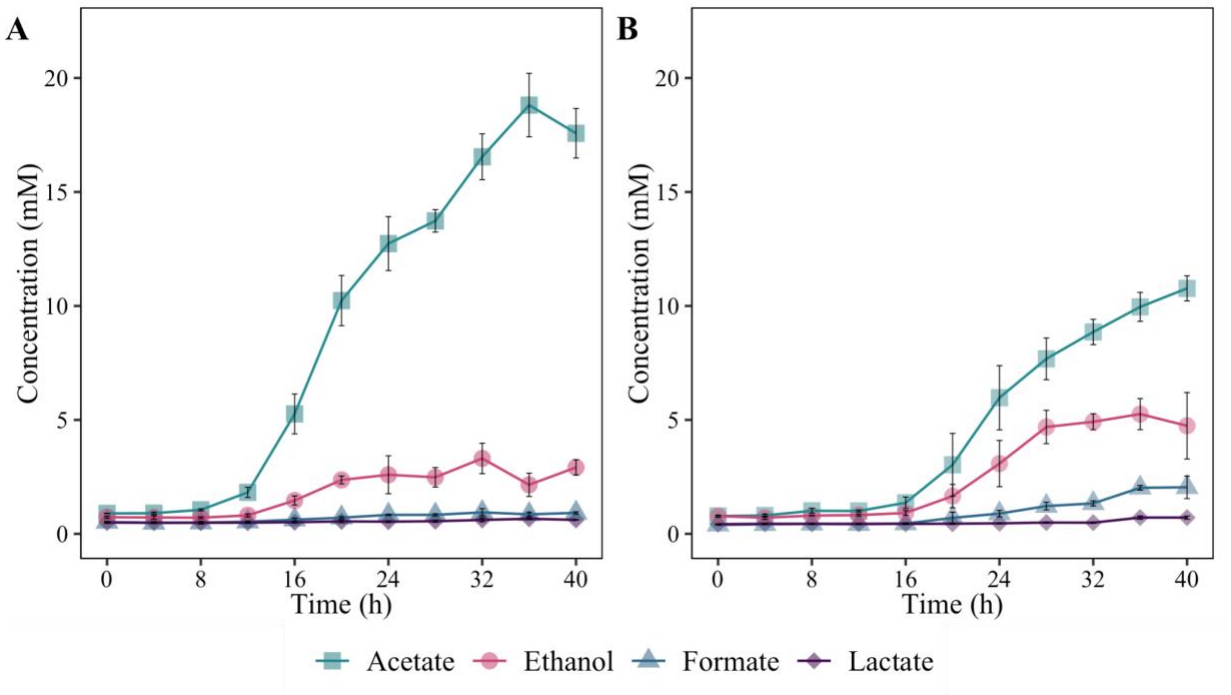

Figure 6. Detected concentrations of organic end-products in *C. thermocellum* and *M. marburgensis* co-culture (A) and *C. thermocellum* monoculture (B) when grown with 2 g/L cellulose. Each data point represents the mean of three biological replicates and error bars denote the standard deviations.

Table 3. Concentrations of fermentation end-products and residual cellulose, and calculated carbon balance and O/R index at the end of fermentation (40h) when cultures were grown with 2 g/L cellulose.

	C. thermocellum (in mM)		***C. thermocellum* + *M. marburgensis*** (in mM)	
	Mean	SD[c]	Mean	SD[c]
Detected H_2	17.48	0.562	0.902	0.312
Calculated H_2[a]	-		21.42	0.137
Detected CO_2	12.38	0.556	10.15	0.291
Calculated CO_2[a]	-		15.28	0.255
CH_4	0		5.130	0.092
Lactate	0.715	0.067	0.612	0.010
Fomate	2.043	0.496	0.922	0.048
Acetate	10.77	0.549	17.57	1.085
Ethanol	4.742	1.458	2.916	0.335
Residual cellulose (as glucose equivalent)	0.064	0.017	0.0141	0.002
Carbon balance[b]	0.704	0.095	0.849	0.072
O/R index[b]	1.001	0.120	1.155	0.034

[a]In *C. thermocellum* + *M. marburgensis* co-culture, calculated H_2 and CO_2 were based on the detected concentrations of CH_4 produced by *M. marburgensis* at the end of fermentation (40 h pi); 1 mole of CH_4 is equivalent to 1 mole of CO_2 and 4 moles of H_2.

[b]In *C. thermocellum* + *M. marburgensis* co-culture, carbon balance and O/R index were determined using the detected concentrations of lactate, formate, acetate, ethanol and residual cellulose, and the calculated concentrations of H_2 and CO_2 based on CH_4.

[c]SD = standard deviation.

3.3 Alternate end-products at high carbon concentrations

C. thermocellum in monocultures and in co-cultures with *M. marburgensis* were grown in 10 g/L of Avicel while *M. marburgensis* monocultures were grown on 80% H_2 and 20% CO_2 to determine the effect of high initial carbon concentration on the end-product profile of *C. thermocellum* and *M. marburgensis*. Detected metabolite concentrations at the beginning of fermentation (0 h), exponential phase (20 h pi), and stationary phase (44 h pi) is shown in Figure 7 and 8. In addition to the typical fermentation end-products of *C. thermocellum* (Appendix Figure 14), amino acids and TCA cycle intermediates were also detected in *C. thermocellum* grown in the presence and absence of *M. marburgensis*. *C. thermocellum* in monocultures and co-cultures with *M. marburgensis* produced all of the different detected amino acids during the exponential phase and an increase in concentrations was observed by the end of fermentation, with the exception of methionine. An increase over time in fumarate, α-hydroxyglutarate and α-ketoglutarate levels was observed in both *C. thermocellum* cultures while an increase over time in succinate levels was only observed in *C. thermocellum* co-cultures with *M. marburgensis*. In the *M. marburgensis* monocultures, secretion of alanine, isoleucine, proline, glycine, glutamate, and methionine in trace amounts was observed by 44 h pi while succinate levels reached only 0.024 mM (± 0.004).

The distribution of typical and alternate end-products detected for each culture during the stationary phase are presented as the concentration of equivalent carbon is shown in Figure 9. The most predominant alternate end-product detected in *C. thermocellum* monocultures and co-cultures is valine. However, a 50% reduction in valine levels was observed in the co-cultures relative to *C. thermocellum* monocultures. Higher levels of succinate (1.1 mM of carbon) were also detected in the co-cultures compared to monocultures of *C. thermocellum* (0.04 mM of

carbon) and *M. marburgensis* (0.10 mM of carbon). Lower levels of metabolites were detected in *M. marburgensis* monocultures, with alanine (0.18 mM of carbon) being secreted at the highest level.

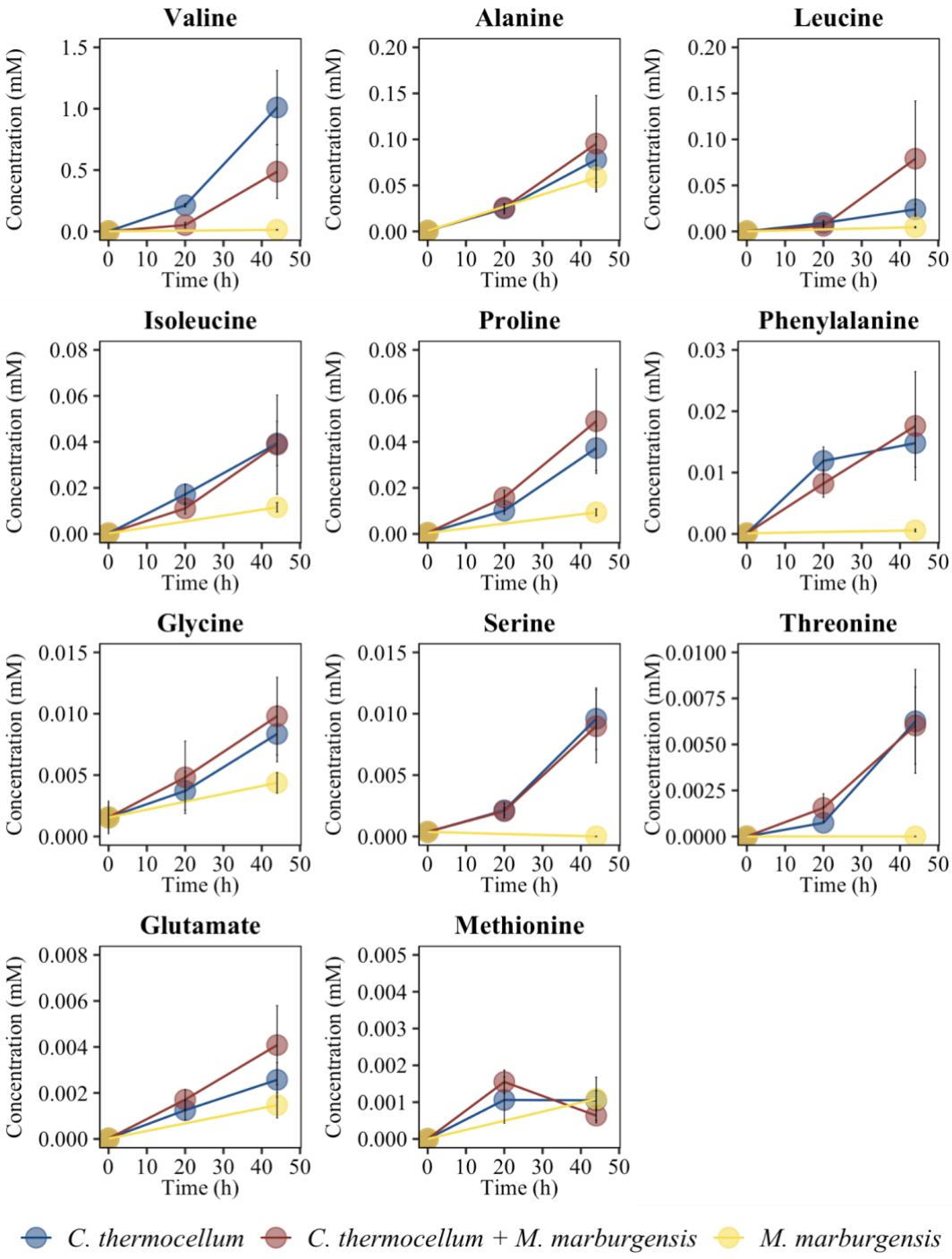

Figure 7. Detected concentrations of amino acids in *C. thermocellum* and *M. marburgensis* monocultures and co-culture at high carbon loading (10 g/L Avicel). Each data point represents the mean of three biological replicates and error bars denote the standard deviations. Note the differences in concentration scales on the y axes.

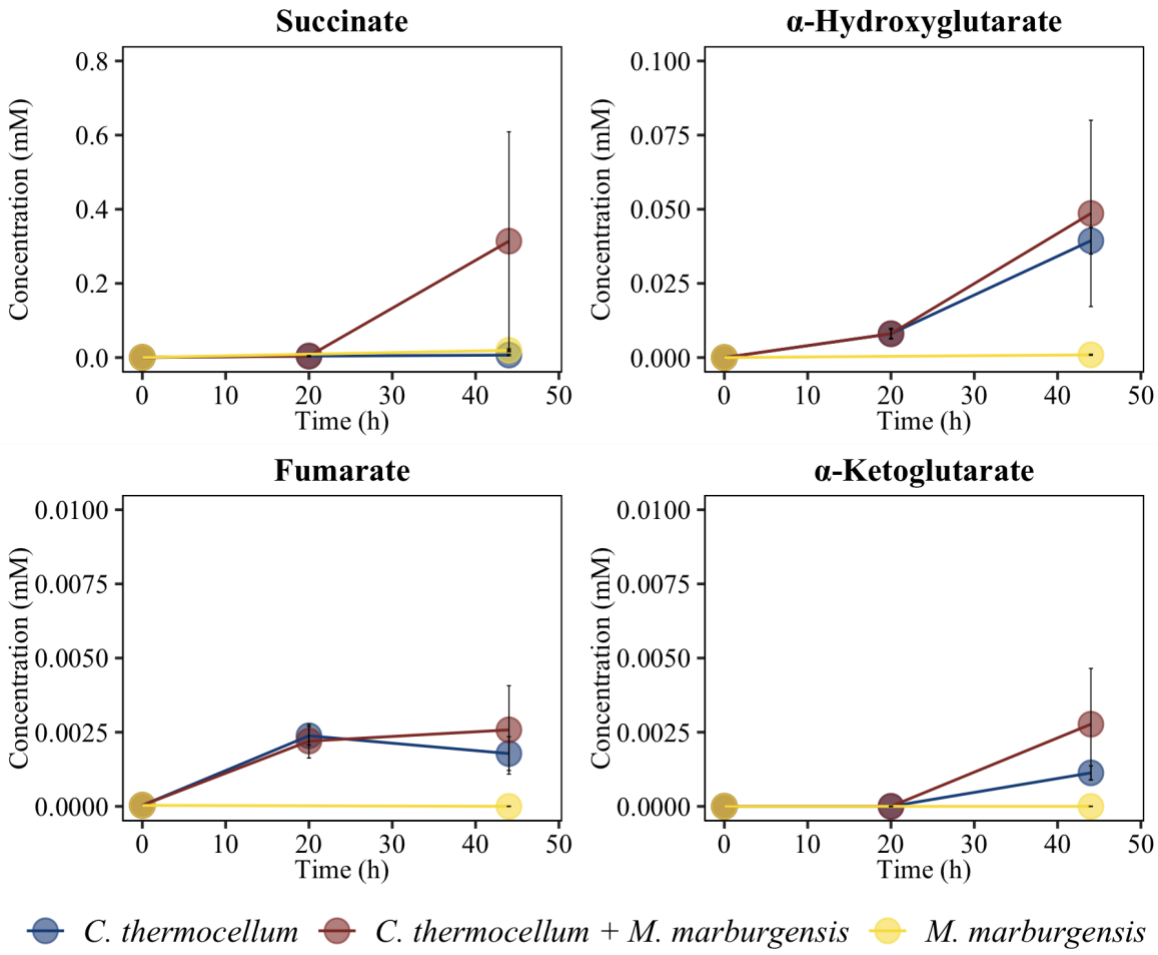

Figure 8. Detected concentrations of succinate, α-hydroxyglutarate, fumarate, and α-ketoglutarate in *C. thermocellum* and *M. marburgensis* monocultures and co-culture at high carbon loading (10 g/L Avicel). Each data point represents the mean of three biological replicates and error bars denote the standard deviations. Note the differences in concentration scales on the y axes.

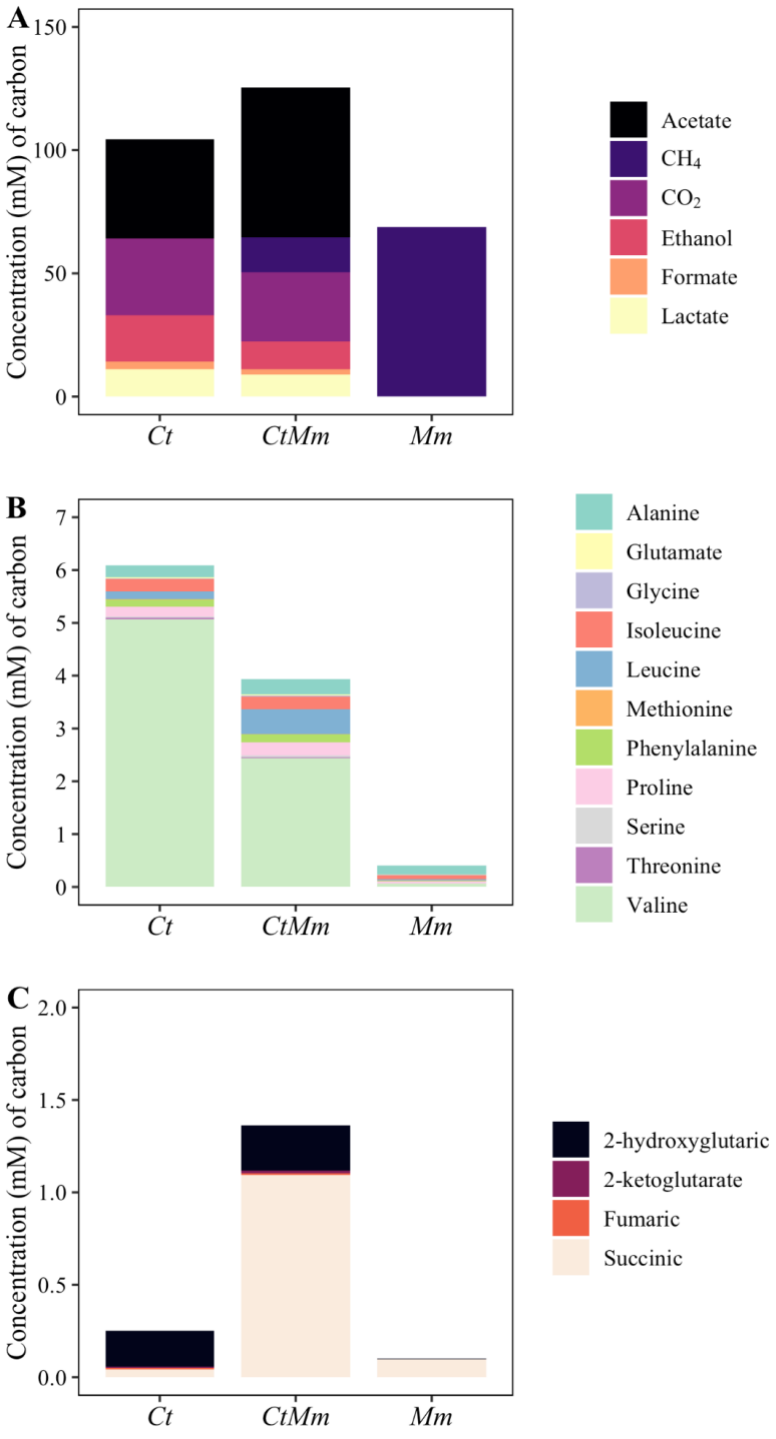

Figure 9. Distribution of typical fermentation end-products (A), amino acids (B), and TCA cycle intermediates (C) at high initial carbon concentrations. Samples were taken at the end of fermentation (44h) and are presented as concentrations of equivalent carbon. *Ct = C. thermocellum*

monoculture, *CtMm = C. thermocellum + M. marburgensis* co-culture, *Mm = M. marburgensis* monoculture. Data represent the mean of three biological replicates. Note the differences in concentration scales on the y axes.

3.4 Cell interaction in co-culture

Potential *C. thermocellum* and *M. marburgensis* interaction in co-culture was investigated via measurement of cell concentration on the cotton and fermentation broth (supernatant), and examination of the cotton samples via scanning electron microscopy (SEM). The distribution of *C. thermocellum* and *M. marburgensis* cells on the cotton and supernatant is shown in Figure 10. More *C. thermocellum* cells appear to be on the cotton, presumably as part of the biofilm, than in the supernatant in both the monocultures and the co-cultures with *M. marburgensis*. Significantly more *M. marburgensis* cells ($P = 0.0017$) were found present in the supernatant compared to the cotton in monocultures as *M. marburgensis*, unlike *C. thermocellum*, does not bind to and form a biofilm on cellulosic substrates. However, the distribution of *M. marburgensis* cells on the cotton and the supernatant is about the same in the co-culture with *C. thermocellum*. The distribution of cells, primarily *M. marburgensis*, detected on the cotton relative to the supernatant is not sufficient to suggest that *M. marburgensis* physically interacts with *C. thermocellum*.

Cells on the cotton were observed via SEM, and measurements of gas and pH were also taken to determine the phase of growth of the cultures. A high density of cells is observed and appear to have arranged themselves in a single layer with little overlap on the cotton fibres in both the *C. thermocellum* monoculture (Figure 11A) and the co-culture with *M. marburgensis* (Figure 11C). Minimal H_2 is detected along with CH_4 production in *C. thermocellum* in co-culture with *M. marburgensis*, indicating that *M. marburgensis* is present and continuously oxidizing H_2 produced

by *C. thermocellum* (Appendix Figure 15B). However, very few cells were observed on the cotton from *M. marburgensis* monocultures (Figure 11B) despite the detected high cell concentrations and metabolic activity, indicated by CH_4 production and a decrease in H_2 and CO_2 (Appendix Figure 15C). *C. thermocellum* cells in monoculture appear shorter in length (3-10 µm) than *M. marburgensis* cells in monoculture (8-20 µm). Cells in the co-culture range from 5-20 µm in length and many appear elongated with terminal sporangia. *C. thermocellum* and *M. marburgensis* cells are difficult to differentiate in SEM images due to their similarities in shape and length. Confocal scanning microscopy in conjunction with fluorescence staining can be utilized to distinguish *C. thermocellum* cells from *M. marburgensis* cells in co-culture and to observe potential cell interaction (Dumitrache et al., 2013).

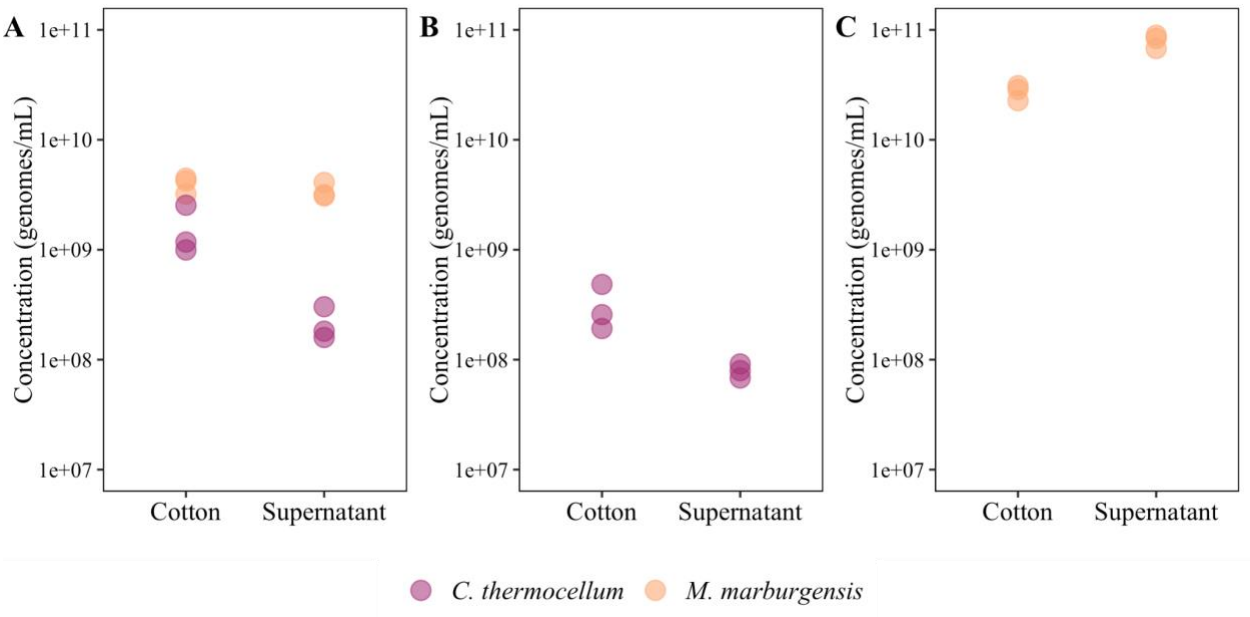

Figure 10. Distribution of *C. thermocellum* and *M. marburgensis* cells on cotton and in the supernatant du*ring mid-expone*ntial phase (24 h pi). *C. thermocellum* and *M. marburgensis* co-cultures (A), *C. thermocellum* monocultures (B), and *M. marburgensis* monocultures (C). Each data point represents one biological replicate from each culture condition.

A

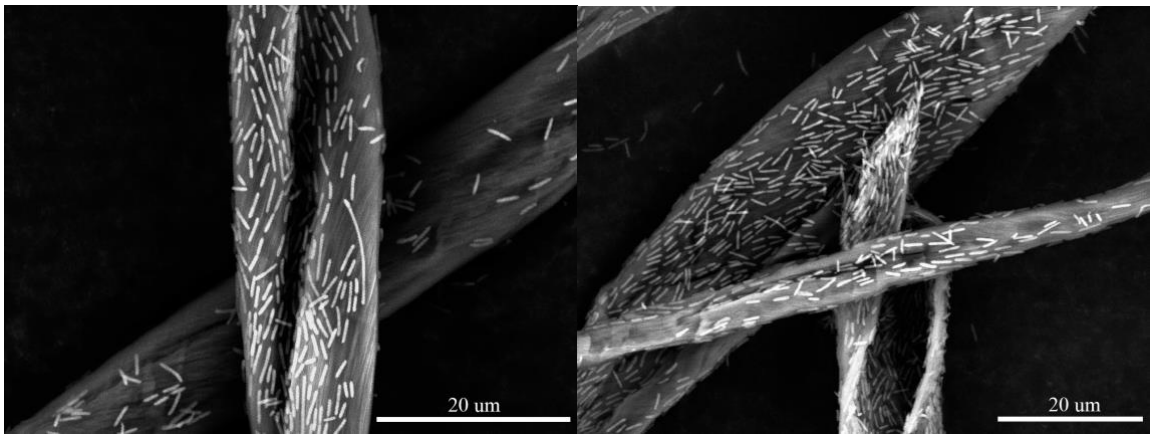

B

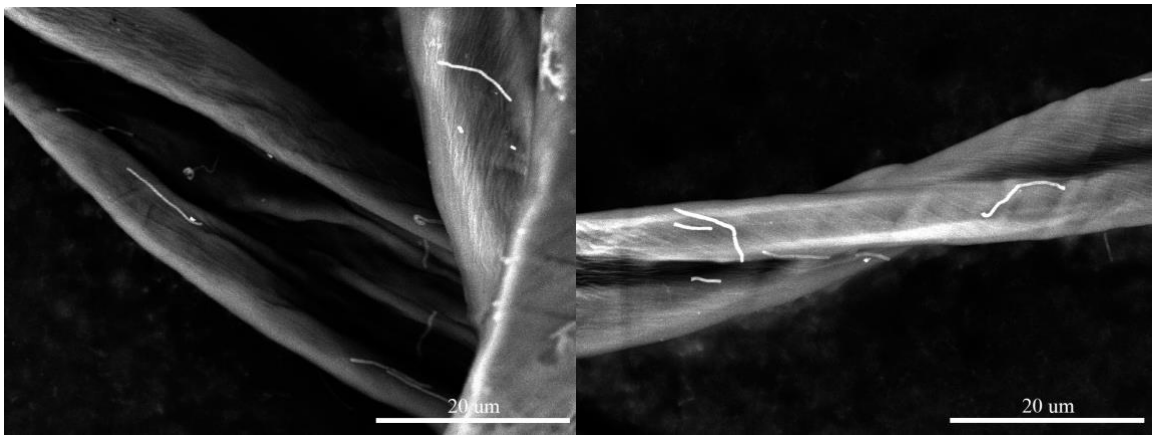

C

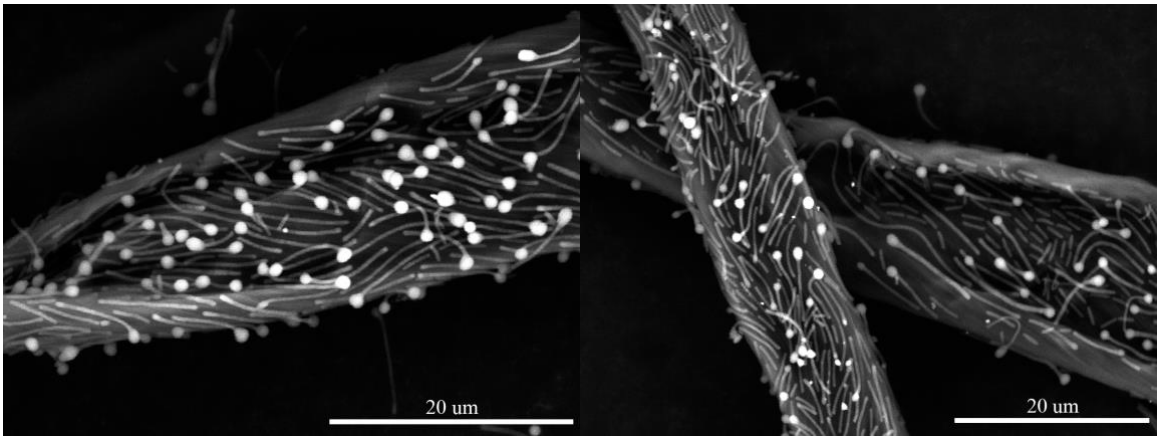

Figure 11. Representative SEM images of *C. thermocellum* and *M. marburgensis* monocultures and co-cultures grown on cotton threads. *C. thermocellum* in monoculture (A), *M. marburgensis* in monoculture (B), and *C. thermocellum* and *M. marburgensis* in co-culture (C) taken during mid-exponential phase (24 h pi).

3.5 H_2ase gene expression in *C. thermocellum*

The transcription of the four genes encoding the catalytic subunits of H_2ases in *C. thermocellum* was assessed when grown in the presence of *M. marburgensis*, in which H_2 produced from cellulose fermentation is continuously consumed by *M. marburgensis* (Figure 12). RT-qPCR was used to determine the gene expression of *C. thermocellum* in co-culture with *M. marburgensis* relative to the gene expression of *C. thermocellum* in monoculture, where H_2 was able to accumulate. A decrease in expression of the three [FeFe] H_2ase genes (Cthe_0342, Cthe_0430, and Cthe_3003) was observed. The most significant change was observed in the putative bifurcating H_2ase (Rydzak et al., 2012), Cthe_0430, which had a 10-fold decrease ($P < 0.001$) in gene expression and was the most down-regulated. The other putative bifurcating H_2ase (Rydzak et al., 2012), Cthe_0342, was also downregulated but only by 2-fold ($P < 0.001$). The NADPH-dependent H_2ase, Cthe_3003, had a 1.5-fold decrease ($P < 0.001$) in gene expression. Whereas no significant change ($P = 0.46$) in expression was observed for the Ech-like [NiFe] H_2ase, Cthe_3020.

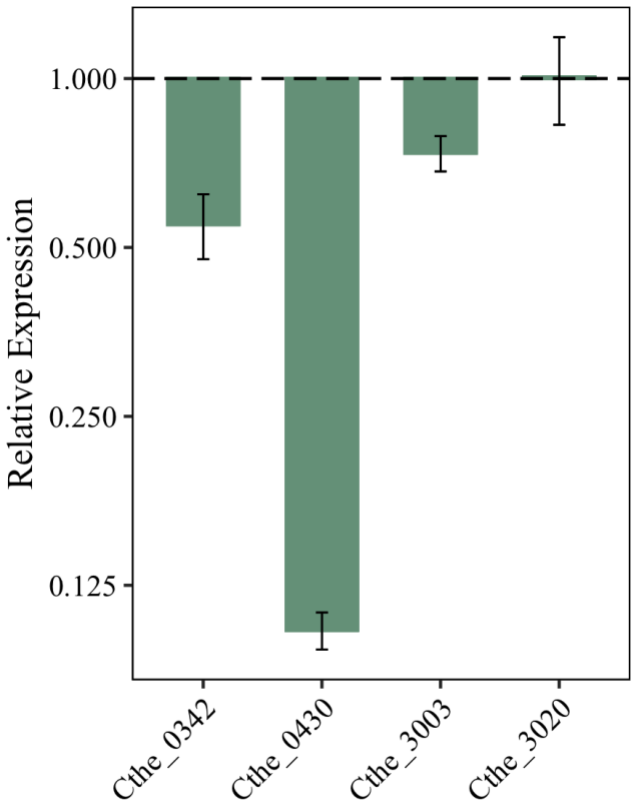

Figure 12. Expression of H_2ase genes in *C. thermocellum* in co-culture with *M. marburgensis* relative to *C. thermocellum* in monoculture during the mid-exponential phase of growth (16 h pi) with 2 g/L of cellulose. cDNA from *C. thermocellum* in monoculture was used as the calibrator and *recA* was used as the normalizer gene.

Chapter 4: DISCUSSION

4.1 Growth and end-product synthesis of *C. thermocellum* in the presence and absence of *M. marburgensis*

Considering the literature outlined in the introduction, we hypothesized that growing *C. thermocellum* in the presence of *M. marburgensis* will alter the growth and fermentation end-product formation of *C. thermocellum*. *M. marburgensis* will act as an 'electron sink' for *C. thermocellum* by continuously consuming H_2 and could even alleviate the redox imbalance that occurs during growth on high cellulose loading and high end-product accumulation. To test our hypotheses, we directly compared the growth, cellulose hydrolysis, and end-product synthesis of *C. thermocellum* grown in monocultures and in co-cultures with *M. marburgensis* on 2 g/L of cellulose, in which minimal H_2 levels were maintained. We also grew *C. thermocellum* monocultures and co-cultures with *M. marburgensis* in minimal media with high cellulose concentration (10 g/L) to directly compare secreted metabolites from overflow metabolism in *C. thermocellum*.

Consistent with the previous work of Weimer and Zeikus (1977), a shorter lag period, earlier initiation of cellulolysis, and a dramatic shift in end-product formation were observed in *C. thermocellum* grown in the presence of *M. marburgensis* compared to *C. thermocellum* grown in monocultures. The continuous H_2 and CO_2 consumption by *M. marburgensis* in co-culture resulted in a significant change in the formation of acetate, ethanol and formate. Electrons in the form of reduced co-factors, such as reduced Fd and NADH, are disposed towards the formation of more H_2 (Carere et al., 2014). Reduced Fd does not accumulate therefore there is no bottleneck at the PFOR, and flux from the pyruvate branch point is directed away from PFL for formate production and towards PFOR for acetyl-CoA, CO_2 and reduced Fd production (Rydzak et al., 2012). Less

electron flux is directed towards ethanol formation, resulting in more acetyl-CoA being directed towards acetate formation, which is associated with ATP production (Rydzak et al., 2012). Although the growth rate of *C. thermocellum* in co-culture with *M. marburgensis* did not differ from that of *C. thermocellum* in monoculture, as reported in previous studies (Weimer & Zeikus, 1977; Collet et al., 2005), we observed a faster rate of cellulose hydrolysis in the co-culture compared to the monoculture. The increased rate of cellulose degradation is presumably a consequence of the utilization of additional ATP through the conversion of acetyl-CoA to acetyl-P to acetate plus ATP associated with the observed increase in acetate formation.

The free amino acids we detected in this study are consistent with those reported in previous studies (Ellis et al., 2012; Holwerda et al., 2014). Valine was predominantly produced by *C. thermocellum* in both monocultures and co-cultures but a significant reduction in valine levels was observed in the co-cultures compared to the monocultures. Excess electron flux under high carbon concentrations could be directed towards the production of free amino acids, which are reduced end-products (Kengen & Stams, 1994). The observed decrease in valine levels in the co-cultures could be a result of *M. marburgensis* acting as an 'electron sink' for *C. thermocellum* by continuously consuming electrons in the form of H_2. The biosynthesis pathways of the free amino acids from pyruvate have not been completely resolved and further investigation of the genome and proteome of *C. thermocellum* are required.

We also detected TCA intermediates, such as succinate, α-hydroxyglutarate, fumarate, and α-ketoglutarate, in both *C. thermocellum* monocultures and co-cultures. The key difference between *C. thermocellum* monocultures and co-cultures is the production of significant amounts of succinate in the co-culture. *M. marburgensis* in monoculture produced significantly less succinate than the *C. thermocellum* and *M. marburgensis* co-culture. Due to the electron flux in *C.*

thermocellum being directed towards *M. marburgensis* and converted to CH_4, excess carbon may be directed towards the production of more oxidized end-products, such as succinate. Succinate is a metabolic intermediate of the TCA cycle and although *C. thermocellum* does not have a complete TCA cycle, it has been reported to produce TCA cycle intermediates, such as oxaloacetate, malate and fumarate, as intermediates of other pathways (Ellis et al., 2012; Rydzak et al., 2012; Holwerda et al., 2014). To our knowledge, there have been no previous reports of *C. thermocellum* secreting succinate. Nevertheless, it is one of the main fermentation end-products of a close relative, *Clostridium thermosuccinogenes* (Koendjbiharie et al., 2018). In *C. thermosuccinogenes*, the proposed pathway for the formation of succinate from PEP is via (i) PEP carboxykinase, (ii) malate dehydrogenase, (iii) fumarate hydratase, and (iv) fumarate reductase (Koendjbiharie et al., 2018). There is no annotated fumarate hydratase or fumarate reductase in the genome of *C. thermocellum* but further investigation of its genome may resolve pathways involved in the formation of fumarate and succinate.

4.2 *C. thermocellum* and *M. marburgensis* interaction in co-culture

Based on our findings for the first objective of this thesis that was presented in the results, we hypothesized that *C. thermocellum* and *M. marburgensis* are interacting in close proximity to each other in order to efficiently facilitate interspecies hydrogen transfer at low H_2 partial pressures. To test this hypothesis, we grew cultures on cotton, which allowed us to separate biofilm cells and cells that are in close physical contact with *C. thermocellum* from planktonic cells in the supernatant. We also sought to describe the characteristics of the adhered cells on the cotton through scanning electron microscopy.

If *M. marburgensis* is directly bound to (Thoma et al., 2008) or co-aggregate with (Ishii et al., 2005) *C. thermocellum* cells, a significantly higher concentration of *M. marburgensis* cells

would be on the cotton compared to the supernatant when it is grown in co-culture with *C. thermocellum*. We observed that there is an approximately equal distribution of *M. marburgensis* cells on the cotton and in the supernatant in co-culture with *C. thermocellum*. *M. marburgensis*, unlike *C. thermocellum*, do not adhere to or form a biofilm on cellulosic substrates, such as cotton (Wasserfallen et al., 2000). Interestingly, even though there are significantly more *M. marburgensis* cells in the supernatant compared to the cotton when grown in monoculture, a considerable amount of *M. marburgensis* cells were still detected on the cotton. We think that this may be due to sample preparation for cell enumeration, in which *M. marburgensis* cells in the supernatant or the liquid-gas interphase may be getting on the cotton upon isolation from the supernatant. Comparing the concentration of *M. marburgensis* cells on the cotton and the supernatant is not sufficient to determine if direct physical contact between *M. marburgensis* and *C. thermocellum* is occurring in co-culture.

The morphology of both *C. thermocellum* and *M. marburgensis* cells in monocultures observed in this study is consistent with previous studies (Dumitrache et al., 2013; Wasserfallen et al., 2000). The observed biofilm structure of *C. thermocellum* on the cotton in co-cultures is consistent with observations of Dumitrache et al. (2013) of *C. thermocellum* during late logarithmic phase that was grown in monoculture. In the SEM images of the cotton from co-cultures, *M. marburgensis* cells were difficult to differentiate from vegetative *C. thermocellum* cells, which appear longer due to the formation of long chains or cell elongation (Dumitrache et al., 2013). A combination of probes specific to each microbe and higher microscopic resolution may be able to differentiate *M. marburgensis* and *C. thermocellum* cells if they are interconnected in co-culture. However, if cells are in close proximity to each other but not directly bound, sample preparation needs to be considered as *M. marburgensis* cells can be washed away. Our findings

suggest that direct interaction between *C. thermocellum* and *M. marburgensis* in co-culture may not occur though further investigation using techniques that can definitively differentiate the two species and reveal the mode of interaction, if it occurs, is required.

4.3 H_2ase gene expression in *C. thermocellum*

Considering results from the previous work of Carere et al. (2014) and the ability of *M. marburgensis* to maintain a low H_2 partial pressure in the co-cultures, we hypothesized that transcription of *C. thermocellum* H_2ases will increase and may be regulated in response to H_2 levels. To our knowledge, low H_2 levels in the gas and liquid phases have not been achieved using mechanical methods, such as gas sparging, due to the supersaturation of dissolved H_2 during fermentation (Kraemer and Bagley, 2006; Carere et al., 2014, Blunt et al., 2015). To test our hypothesis, we investigated the gene expression levels of H_2ases in *C. thermocellum* grown in co-culture with *M. marburgensis* relative to *C. thermocellum* grown in monoculture via RT-qPCR.

Interestingly, the transcription of the large subunits of all three [FeFe] H_2ases (Cthe_0342, Cthe_0430 and Cthe_3003) significantly decreased in response to continuous H_2 removal by *M. marburgensis*. Rydzak et al. (2012) suggested that H_2 production in *C. thermocellum* is primarily via a bifurcating system, involving Fd-dependent H_2ase (Cthe_0430) and NADH-dependent H_2ase (Cthe_0342), that can overcome the thermodynamic barriers associated with NADH oxidation to H_2 (Lamed et al., 1988; Schut & Adams, 2009). We think that due to *M. marburgensis* continuously consuming H_2 produced by *C. thermocellum*, there is no thermodynamic barrier impeding the oxidation of NADH and, therefore, increased expression of the Fd-dependent H_2ase (Cthe_0430) and NADH-dependent H_2ase (Cthe_0342) genes are not necessary. The NADH-dependent H_2ase (Cthe_0342) does not need the reducing power of Fd to oxidize NADH to H_2 due to the low H_2 partial pressure and hence why there is a significantly lower expression (10-fold) of

the Fd-dependent H_2ase (Cthe_0430). The NADPH-dependent H_2ase gene (Cthe_3003) of *C. thermocellum* is adjacent to a gene (Cthe_3004) that is similar to the NAPDH-binding subunit of glutamate synthase, suggesting it may form a dimer that can produce NADPH from H_2 (Calusinska et al., 2010). Since H_2 produced by *C. thermocellum* does not accumulate in co-culture, there is less available H_2 for the NADPH-dependent H_2ase (Cthe_3003) to reoxidize. Transcription of the large subunit of the Ech-like [NiFe] H_2ase (Cthe_3020) did not change in response to continuous H_2 removal, which is in agreement with the findings of Carere et al. (2014) when *C. thermocellum* cultures were sparged with N_2. Our work suggests that *C. thermocellum* [FeFe] H_2ases may be transcriptionally regulated by H_2 levels and thermodynamic considerations dictate the observed changes in fermentation end-product profile. It appears that *M. marburgensis*, in this instance, may be dictating the thermodynamics in *C. thermocellum* metabolism.

Chapter 5: CONCLUSION AND FUTURE DIRECTIONS

Applications of emerging technologies, such as microbial fermentation with low-cost and sustainable substrates, to transition away from fossil fuels are required to combat the accelerating effects of climate change. Lignocellulosic biomass can be converted to biofuels and other high-value chemicals via consolidated bioprocessing using microbes that can simultaneously hydrolyze and ferment substrates (Parisutham et al., 2014). *Clostridium thermocellum* is one of the most well-characterized and promising candidates for this process (Lu et al., 2006). However, industrial-scale production of high-value chemicals, such as ethanol for transportation fuel, using *C. thermocellum* is currently not feasible due to low product yield (Lynd et al., 2017). Investigation of metabolic relationships formed by *C. thermocellum* with other microbes in nature, such as methanogens, may enhance our understanding of cellular bioenergetics and metabolism, which can aid in future engineering efforts to increase product yield in *C. thermocellum*.

The aim of our work was to further fill the gaps in our knowledge of the metabolic pathways in *C. thermocellum*, especially the carbon and electron overflow pathways observed in the presence of high excess cellulose in stationary phase, by investigating changes in its physiology when grown in co-culture with *M. marburgensis*. We demonstrated that *M. marburgensis* acts as an 'electron sink' for *C. thermocellum* and may dictate the thermodynamics in *C. thermocellum* metabolism when grown on cellulosic substrates. This resulted in drastic changes in the fermentation and overflow metabolism end-product profile in *C. thermocellum*. Surprisingly, transcription of *C. thermocellum* Fd-dependent H_2ase (Cthe_0430), NADH-dependent H_2ase (Cthe_0342) and NADH-dependent H_2ase (Cthe_0342) decreased with continuous H_2 consumption by *M. marburgensis*. This led us to suggest that *C. thermocellum* H_2ases, except for the [NiFe] Ech H_2ase, may be transcriptionally regulated by H_2 levels. Although changes in

metabolism and H_2ase transcription were observed, the mode of interaction between *C. thermocellum* and *M. marburgensis* was not determined due to insufficient evidence. However, the presence of *M. marburgensis* had less of an impact on carbon overflow than expected. There was a reduction in valine production, which coincided with an increase in the production of more oxidized dicarboxylic acids, such as succinate.

Future work would involve the investigation of intracellular metabolite (e.g. NADH, Fd, ATP, pyruvate, etc.) levels in *C. thermocellum* in the presence and absence of *M. marburgensis* as it may further improve our understanding of the modulation of metabolite synthesis and regulation of H_2ase transcription. Transcriptomic analysis using microarrays can also be performed to investigate changes in expression of other genes associated with central metabolism and fermentation in *C. thermocellum* in the presence and absence of *M. marburgensis*, and to confirm our findings in this thesis. Additionally, further investigation of the genome of *C. thermocellum* and enzyme characterization can aid in understanding the mechanism of amino acid and TCA cycle intermediate synthesis in *C. thermocellum*.

APPENDIX

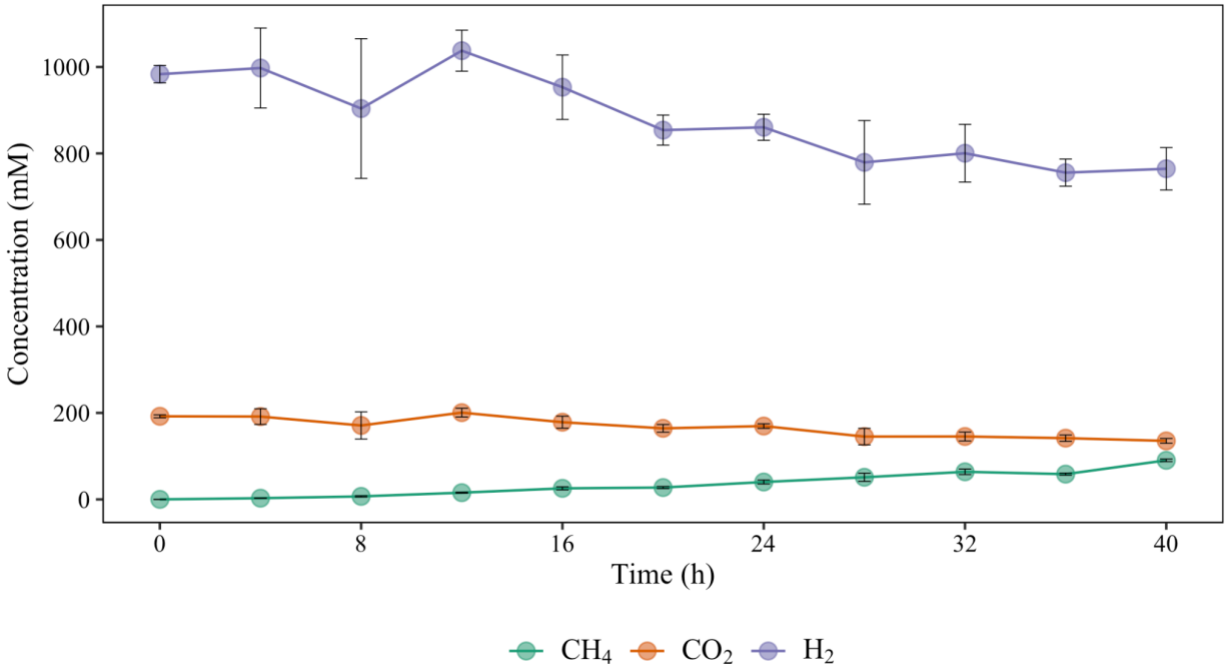

Figure 13. Gas consumption and production in *M. marburgensis* monoculture grown on minimal media with a mixture of 80% H_2 and 20% CO_2. Each data point represents the mean of three biological replicates and error bars denote the standard deviations.

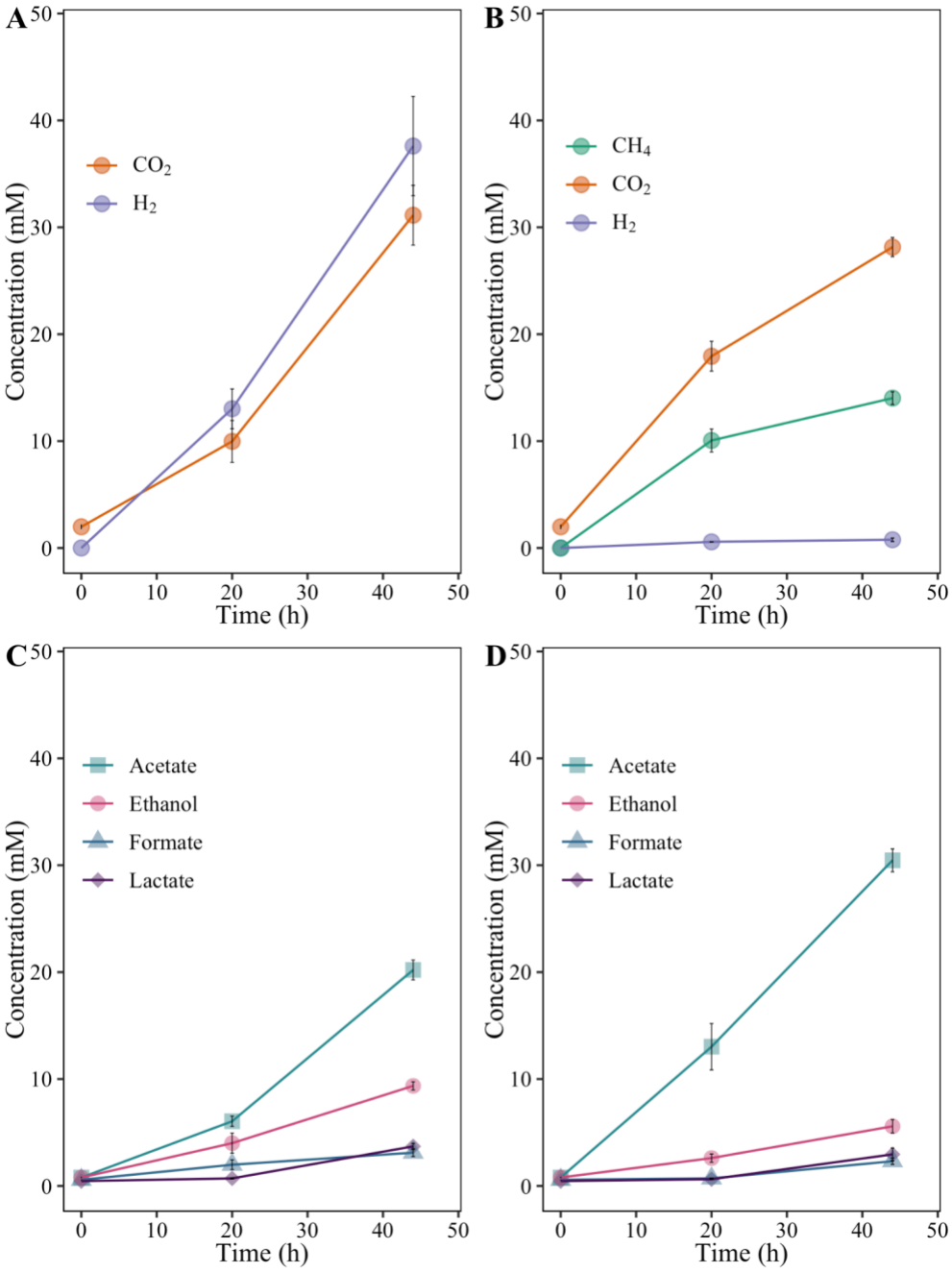

Figure 14. *C. thermocellum* fermentation end-products in monoculture and co-culture with *M. marburgensis* at high carbon loading (10 g/L Avicel). Gas end-products in *C. thermocellum* monoculture (A) and *C. thermocellum* + *M. marburgensis* co-culture (B); Liquid end-products in *C. thermocellum* monoculture (C) and *C. thermocellum* + *M. marburgensis* co-culture (D). Each

data point represents the mean of three biological replicates and error bars denote the standard deviations.

A

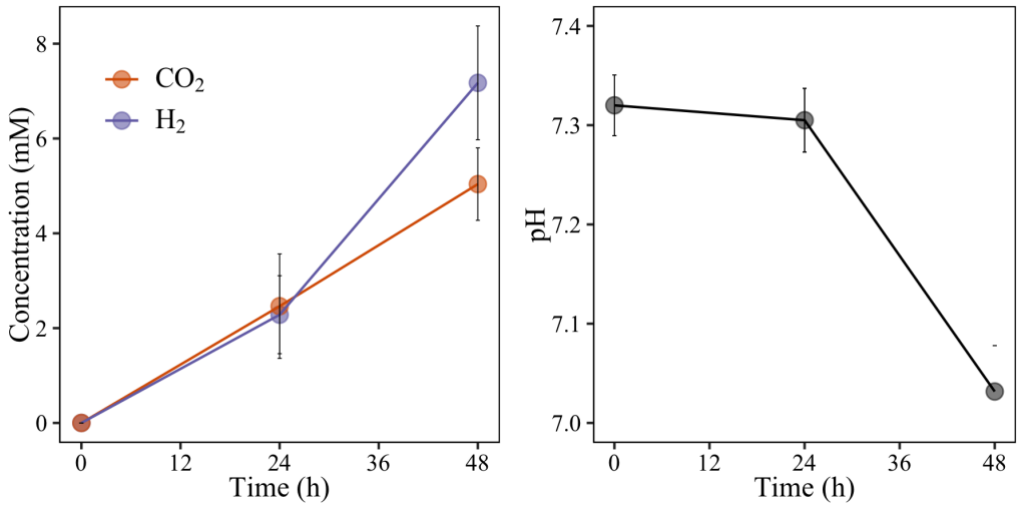

B

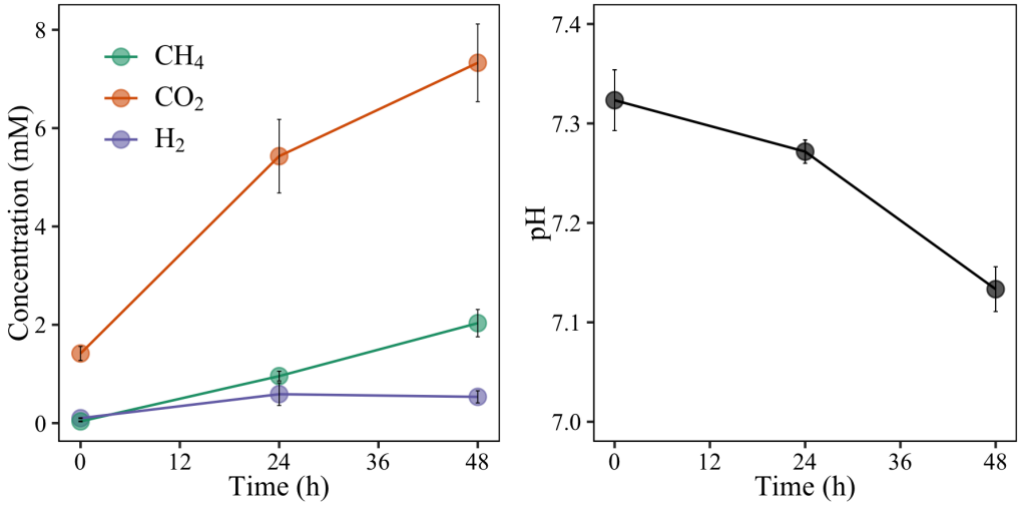

C

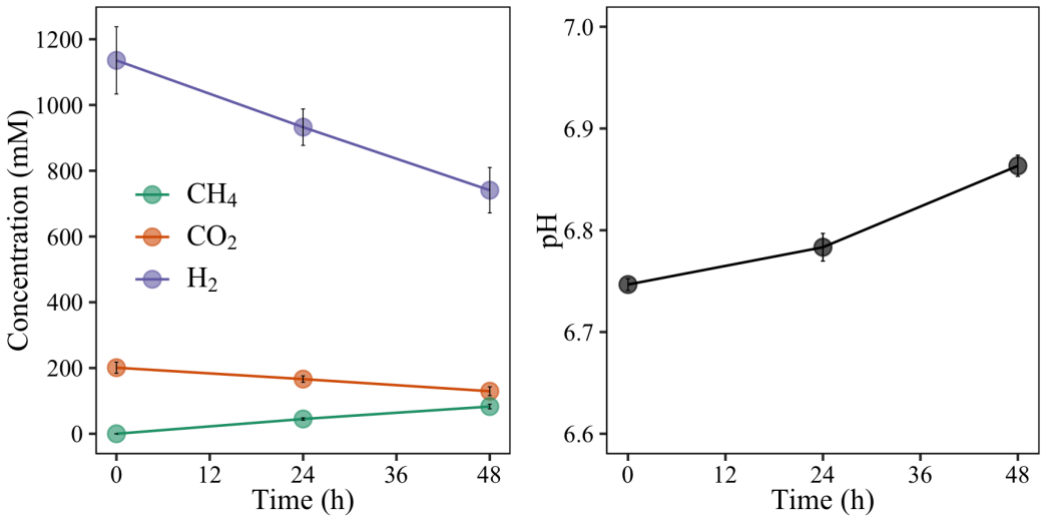

Figure 15. Gaseous end-products and pH in *C. thermocellum* monoculture (A), *C. thermocellum* + *M. marburgensis* co-culture (B), and *M. marburgensis* monoculture (C) on 2 g/L of untreated cotton. Each data point represents the mean of three biological replicates and error bars denote the standard deviations.

Table 4. Calculated carbon balance and O/R index in *C. thermocellum* monoculture and *C. thermocellum* and *M. marburgensis* co-culture grown with 2 g/L cellulose.

Time (h pi)	*C. thermocellum*		*C. thermocellum* + *M. marburgensis*	
	Carbon balance	**O/R index**	**Carbon balance[a]**	**O/R index[a]**
28	0.70 (0.06)	0.99 (0.06)	0.74 (0.04)	1.18 (0.04)
32	0.68 (0.04)	0.94 (0.08)	0.85 (0.08)	1.13 (0.02)
36	0.69 (0.03)	0.92 (0.05)	0.88 (0.06)	1.22 (0.05)
40	0.70 (0.10)	1.00 (0.12)	0.85 (0.07)	1.16 (0.03)

[a]In *C. thermocellum* + *M. marburgensis* co-culture, carbon balance and O/R index were determined using the detected concentrations of lactate, formate, acetate, ethanol and residual cellulose, and the calculated concentrations of H_2 and CO_2 based on CH_4.

REFERENCES

Ait, N., Creuzet, N., & Cattaneo, J. (1982). Properties of glucosidase purified from *Clostridium thermocellum*. *Microbiology*, *128*(3), 569–577. https://doi.org/10.1099/00221287-128-3-569

Akinosho, H., Yee, K., Close, D., & Ragauskas, A. (2014). The emergence of *Clostridium thermocellum* as a high utility candidate for consolidated bioprocessing applications. *Frontiers in Chemistry*, *2*. https://doi.org/10.3389/fchem.2014.00066

Bayer, E. A., Kenig, R., & Lamed, R. (1983). Adherence of *Clostridium thermocellum* to cellulose. *Journal of Bacteriology*, *156*(2), 818–827. https://doi.org/10.1128/jb.156.2.818-827.1983

Bellard, C., Bertelsmeier, C., Leadley, P., Thuiller, W., & Courchamp, F. (2012). Impacts of climate change on the future of biodiversity. *Ecology Letters*, 15, 365– 377. https://doi-org.uml.idm.oclc.org/10.1111/j.1461-0248.2011.01736.x

Biddy, M. J., Scarlata, C., & Kinchin, C. (2016). Chemicals from biomass: a market assessment of bioproducts with near-term potential. *Office of Scientific and Technical Information (OSTI)*. http://dx.doi.org/10.2172/1244312

Biswas, R., Zheng, T., Olson, D. G., Lynd, L. R., & Guss, A. M. (2015). Elimination of hydrogenase active site assembly blocks H_2 production and increases ethanol yield in *Clostridium thermocellum*. *Biotechnology for Biofuels*, *8*(1). https://doi.org/10.1186/s13068-015-0204-4

Blumer-Schuette, S. E., Brown, S. D., Sander, K. B., Bayer, E. A., Kataeva, I., Zurawski, J. V., Conway, J. M., Adams, M. W. W., & Kelly, R. M. (2014). Thermophilic lignocellulose deconstruction. *FEMS Microbiology Reviews*, *38*(3), 393–448. https://doi.org/10.1111/1574-6976.12044

Blunt, W. A., Taillefer, M., Gapes, D. J., Sparling, R., Levin, D. B., & Cicek, N. (2015). Evaluating supersaturation of in situ produced gasses during thermophilic cellobiose fermentation with *Clostridium thermocellum*. *Transactions of the ASABE*, *58*(5), 1149–1157. https://doi.org/10.13031/trans.58.11297

Brown, S. D., Guss, A. M., Karpinets, T. V., Parks, J. M., Smolin, N., Yang, S., Land, M. L., Klingeman, D. M., Bhandiwad, A., Rodriguez, M., Jr., Raman, B., Shao, X., Mielenz, J. R., Smith, J. C., Keller, M., & Lynd, L. R. (2011). Mutant alcohol dehydrogenase leads to improved ethanol tolerance in *Clostridium thermocellum*. *Proceedings of the National Academy of Sciences*, *108*(33), 13752–13757. https://doi.org/10.1073/pnas.1102444108

Burrell, P. C., O'Sullivan, C., Song, H., Clarke, W. P., & Blackall, L. L. (2004). Identification, detection, and spatial resolution of *Clostridium* populations responsible for cellulose degradation in a methanogenic landfill leachate bioreactor. *Applied and Environmental Microbiology*, *70*(4), 2414–2419. https://doi.org/10.1128/aem.70.4.2414-2419.2004

Calusinska, M., Happe, T., Joris, B., & Wilmotte, A. (2010). The surprising diversity of clostridial hydrogenases: a comparative genomic perspective. *Microbiology*, *156*(6), 1575–1588. https://doi.org/10.1099/mic.0.032771-0

Carere, C.R., Rydzak, T., Cicek, N., Levin, D.B., & Sparling, R. (2014). Role of transcription and enzyme activities in redistribution of carbon and electron flux in response to N_2 and H_2 sparging of open-batch cultures of *Clostridium thermocellum* ATCC 27405. *Applied Microbiology and Biotechnology, 98*, 2829-2840

Carere, C. R., Kalia, V., Sparling, R., Cicek, N., & Levin, D. B. (2008). Pyruvate catabolism and hydrogen synthesis pathway genes of *Clostridium thermocellum* ATCC 27405. *Indian Journal of Microbiology*, *48*(2), 252–266. https://doi.org/10.1007/s12088-008-0036-z

Chandra Raj, K., Ingram, L., & Maupin-Furlow, J. (2001). Pyruvate decarboxylase: a key enzyme for the oxidative metabolism of lactic acid by *Acetobacter pasteurianus*. *Archives of Microbiology*, *176*(6), 443–451. https://doi.org/10.1007/s002030100348

Charon, M.H., Volbeda, A., Chabriere, E., Pieulle, L., & Fontecilla-Camps, J. C. (1999). Structure and electron transfer mechanism of pyruvate:ferredoxin oxidoreductase. *Current Opinion in Structural Biology*, *9*(6), 663–669. https://doi.org/10.1016/s0959-440x(99)00027-5

Chowdhury, H., & Loganathan, B. (2019). Third-generation biofuels from microalgae: a review. *Current Opinion in Green and Sustainable Chemistry*, *20*, 39–44. https://doi.org/10.1016/j.cogsc.2019.09.003

Clèries, R., Galvez, J., Espino, M., Ribes, J., Nunes, V., & de Heredia, M.L. (2012). BootstRatio: a web-based statistical analysis of fold-change in qPCR and RT-qPCR data using resampling methods. *Comput Biol Med*, 42(4):438-45. doi: 10.1016/j.compbiomed.2011.12.012. Epub 2012 Jan 24. PMID: 22270228

Collet, C., Gaudard, O., Péringer, P., & Schwitzguébel, J.-P. (2005). Acetate production from lactose by *Clostridium thermolacticum* and hydrogen-scavenging microorganisms in continuous culture: effect of hydrogen partial pressure. *Journal of Biotechnology*, *118*(3), 328–338. https://doi.org/10.1016/j.jbiotec.2005.05.011

Craig, C.L., & Weber, R.S. (1998). Selection costs of amino acid substitutions in ColE1 and ColIa gene clusters harbored by *Escherichia coli*. *Molecular Biology and Evolution*, *15*(6), 774–776. https://doi.org/10.1093/oxfordjournals.molbev.a025981

Dashtban, M., Schraft, H., & Qin, W. (2009). Fungal bioconversion of lignocellulosic residues: opportunities and perspectives. *Int. J. Biol. Sci.* 5, 578-595

Dassa, B., Borovok, I., Lamed, R., Henrissat, B., Coutinho, P., Hemme, C. L., Huang, Y., Zhou, J., & Bayer, E. A. (2012). Genome-wide analysis of *Acetivibrio cellulolyticus* provides a blueprint of an elaborate cellulosome system. *BMC Genomics*, *13*(1). https://doi.org/10.1186/1471-2164-13-210

Demain, A. L., Newcomb, M., & Wu, J. H. D. (2005). Cellulase, clostridia, and ethanol. *Microbiology and Molecular Biology Reviews*, *69*(1), 124–154. https://doi.org/10.1128/mmbr.69.1.124-154.2005

Desvaux, M., Guedon, E., & Petitdemange, H. (2000). Cellulose catabolism by *Clostridium cellulolyticum* growing in batch culture on defined medium. *Applied and Environmental Microbiology*, *66*(6), 2461–2470. https://doi.org/10.1128/aem.66.6.2461-2470.2000

Dumitrache, A., Wolfaardt, G., Allen, G., Liss, S. N., & Lynd, L. R. (2013). Form and function

of *Clostridium thermocellum* biofilms. *Applied and Environmental Microbiology*, *79*(1), 231–239. https://doi.org/10.1128/aem.02563-12

Ellis, L. D., Holwerda, E. K., Hogsett, D., Rogers, S., Shao, X., Tschaplinski, T., Thorne, P., & Lynd, L. R. (2012). Closing the carbon balance for fermentation by *Clostridium thermocellum* (ATCC 27405). *Bioresource Technology*, *103*(1), 293–299. https://doi.org/10.1016/j.biortech.2011.09.128

Faubert, B., Boily, G., Izreig, S., Griss, T., Samborska, B., Dong, Z., Dupuy, F., Chambers, C., Fuerth, B. J., Viollet, B., Mamer, O. A., Avizonis, D., DeBerardinis, R. J., Siegel, P. M., & Jones, R. G. (2013). AMPK is a negative regulator of the Warburg effect and suppresses tumor growth in vivo. *Cell metabolism*, *17*(1), 113–124. https://doi.org/10.1016/j.cmet.2012.12.001

Fellows, C. M., Brown, T. C., & Doherty, W. O. S. (2012). Lignocellulosics as a renewable feedstock for chemical industry: chemicals from lignin. In *Green Chemistry for Environmental Remediation* (pp. 561–610). John Wiley & Sons, Inc. http://dx.doi.org/10.1002/9781118287705.ch18

Froese, A., Schellenberg, J., & Sparling, R. (2019). Enhanced depolymerization and utilization of raw lignocellulosic material by co-cultures of *Ruminiclostridium thermocellum* with hemicellulose-utilizing partners. *Canadian Journal of Microbiology*, *65*(4), 296–307. https://doi.org/10.1139/cjm-2018-0535

Fuchs, G., Stupperich, E., & Thauer, R. K. (1978). Acetate assimilation and the synthesis of alanine, aspartate and glutamate in *Methanobacterium thermoautotrophicum*. *Archives of Microbiology*, *117*(1), 61–66. https://doi.org/10.1007/bf00689352

Fulton, L.M., Lynd, L.R., Körner, A., Greene, N., & Tonachel, L.R. (2015). The need for biofuels as part of a low carbon energy future. *Biofuels, Bioprod Biorefining* 9:476–483. https://doi.org/10.1002/bbb.1559

Guedon, E., Payot, S., Desvaux, M., & Petitdemange, H. (2000). Relationships between cellobiose catabolism, enzyme levels, and metabolic intermediates in *Clostridium cellulolyticum* grown in a synthetic medium. *Biotechnology and Bioengineering*, *67*(3), 327–335. https://doi.org/10.1002/(sici)1097-0290(20000205)67:3<327::aid-bit9>3.0.co;2-u

Ha, S.-J., Galazka, J. M., Rin Kim, S., Choi, J.-H., Yang, X., Seo, J.-H., Louise Glass, N., Cate, J. H. D., & Jin, Y.-S. (2011). Engineered *Saccharomyces cerevisiae* capable of simultaneous cellobiose and xylose fermentation. *Proceedings of the National Academy of Sciences*, *108*(2), 504–509. https://doi.org/10.1073/pnas.1010456108

Hill, J.E., Hemmingsen, S.M., Goldade, B.G., Dumonceaux, T.J., Klassen, J., Zijlstra, R.T., Swee, H.G., Van Kessel, AG. (2005). Comparison of ileum microflora of pigs fed corn-, wheat-, or barley-based diets by chaperonin-60 sequencing and quantitative PCR. *Appl Environ Microbiol* 71:867–875. https://doi.org/10.1128/AEM.71.2.867-875.2005

Hirano, K., Kurosaki, M., Nihei, S., Hasegawa, H., Shinoda, S., Haruki, M., & Hirano, N. (2016).

Enzymatic diversity of the *Clostridium thermocellum* cellulosome is crucial for the degradation of crystalline cellulose and plant biomass. *Scientific Reports*, *6*(1). https://doi.org/10.1038/srep35709

Hoffert, M. I., Caldeira, K., Benford, G., Criswell, D. R., Green, C., Herzog, H., Jain, A. K., Kheshgi, H. S., Lackner, K. S., Lewis, J. S., Lightfoot, H. D., Manheimer, W., Mankins, J. C., Mauel, M. E., Perkins, L. J., Schlesinger, M. E., Volk, T., & Wigley, T. M. (2002). Advanced technology paths to global climate stability: energy for a greenhouse planet. *Science (New York, N.Y.)*, *298*(5595), 981–987. https://doi.org/10.1126/science.1072357

Holwerda, E. K., Olson, D. G., Ruppertsberger, N. M., Stevenson, D. M., Murphy, S. J. L., Maloney, M. I., Lanahan, A. A., Amador-Noguez, D., & Lynd, L. R. (2020). Metabolic and evolutionary responses of *Clostridium thermocellum* to genetic interventions aimed at improving ethanol production. *Biotechnology for Biofuels*, *13*(1). https://doi.org/10.1186/s13068-020-01680-5

Holwerda, E. K., Thorne, P. G., Olson, D. G., Amador-Noguez, D., Engle, N. L., Tschaplinski, T. J., van Dijken, J. P., & Lynd, L. R. (2014). The exometabolome of *Clostridium thermocellum* reveals overflow metabolism at high cellulose loading. *Biotechnology for Biofuels*, *7*(1). https://doi.org/10.1186/s13068-014-0155-1

Hungate, R. E. (1969). Chapter IV A roll tube method for cultivation of strict anaerobes. In *Methods in Microbiology* (pp. 117–132). Elsevier. http://dx.doi.org/10.1016/s0580-9517(08)70503-8

IPCC. (2014). Climate Change 2014: Mitigation of Climate Change: Working Group III Contribution to the Fifth Assessment Report of the Intergovernmental Panel on Climate Change. *Cambridge University Press*, Cambridge, United Kingdom

Ishii, S., Kosaka, T., Hori, K., Hotta, Y., & Watanabe, K. (2005). Coaggregation facilitates interspecies hydrogen transfer between *Pelotomaculum thermopropionicum* and *Methanothermobacter thermautotrophicus*. *Applied and Environmental Microbiology*, *71*(12), 7838–7845. https://doi.org/10.1128/aem.71.12.7838-7845.2005

Islam, R., Cicek, N., Sparling, R., & Levin, D. (2006). Effect of substrate loading on hydrogen production during anaerobic fermentation by *Clostridium thermocellum* 27405. *Applied Microbiology and Biotechnology*, *72*(3), 576–583. https://doi.org/10.1007/s00253-006-0316-7

Islam, R., Cicek, N., Sparling, R., & Levin, D. (2009). Influence of initial cellulose concentration on the carbon flow distribution during batch fermentation by *Clostridium thermocellum* ATCC 27405. *Applied Microbiology and Biotechnology*, *82*(1), 141–148. https://doi.org/10.1007/s00253-008-1763-0

Izquierdo, J. A., Goodwin, L., Davenport, K. W., Teshima, H., Bruce, D., Detter, C., Tapia, R., Han, S., Land, M., Hauser, L., Jeffries, C. D., Han, J., Pitluck, S., Nolan, M., Chen, A., Huntemann, M., Mavromatis, K., Mikhailova, N., Liolios, K., Lynd, L. R. (2012). Complete Genome Sequence of *Clostridium clariflavum* DSM 19732. *Standards in Genomic Sciences*, *6*(1), 104–115. https://doi.org/10.4056/sigs.2535732

Jeswani, H. K., Chilvers, A., & Azapagic, A. (2020). Environmental sustainability of biofuels: A review. *Proceedings of the Royal Society A: Mathematical, Physical and Engineering Sciences*, *476*(2243), 20200351. https://doi.org/10.1098/rspa.2020.0351

Jouzani, G., & Taherzadeh, M. J. (2015). Advances in consolidated bioprocessing systems for bioethanol and butanol production from biomass: a comprehensive review. *Biofuel Research Journal*, 152–195. https://doi.org/10.18331/brj2015.2.1.4

Kaster, A. K., Goenrich, M., Seedorf, H., Liesegang, H., Wollherr, A., Gottschalk, G., & Thauer, R. K. (2011). More than 200 genes required for methane formation from H_2 and CO_2 and energy conservation are present in *Methanothermobacter marburgensis* and *Methanothermobacter thermautotrophicus*. *Archaea (Vancouver, B.C.)*, *2011*, 973848. https://doi.org/10.1155/2011/973848

Kato, S., Haruta, S., Cui, Z. J., Ishii, M., Yokota, A., & Igarashi, Y. (2004). *Clostridium straminisolvens* sp. nov., a moderately thermophilic, aerotolerant and cellulolytic bacterium isolated from a cellulose-degrading bacterial community. *International Journal of Systematic and Evolutionary Microbiology*, *54*(6), 2043–2047. https://doi.org/10.1099/ijs.0.63148-0

Kengen, S. W. M., & Stams, A. J. M. (1994). Formation of l-alanine as a reduced end product in carbohydrate fermentation by the hyperthermophilic archaeon *Pyrococcus furiosus*. *Archives of Microbiology*, *161*(2), 168–175. https://doi.org/10.1007/bf00276479

Koendjbiharie, J. G., Hon, S., Pabst, M., Hooftman, R., Stevenson, D. M., Cui, J., Amador-Noguez, D., Lynd, L. R., Olson, D. G., & van Kranenburg, R. (2020). The pentose phosphate pathway of cellulolytic Clostridia relies on 6-phosphofructokinase instead of transaldolase. *Journal of Biological Chemistry*, *295*(7), 1867–1878. https://doi.org/10.1074/jbc.ra119.011239

Koendjbiharie, J. G., Wiersma, K., & van Kranenburg, R. (2018). Investigating the central metabolism of *Clostridium thermosuccinogenes*. *Applied and Environmental Microbiology*, *84*(13). https://doi.org/10.1128/aem.00363-18

Kraemer, J. & Bagley, D. (2006). Supersaturation of dissolved H_2 and CO_2 during fermentative hydrogen production with N_2 sparging. *Biotechnol* Lett 28(18):1485–1491

Kridelbaugh, D. M., Nelson, J., Engle, N. L., Tschaplinski, T. J., & Graham, D. E. (2013). Nitrogen and sulfur requirements for *Clostridium thermocellum* and *Caldicellulosiruptor bescii* on cellulosic substrates in minimal nutrient media. *Bioresource technology*, *130*, 125–135. https://doi.org/10.1016/j.biortech.2012.12.006

Laforsch, C. & Tollrian, R. (2000). A new preparation technique of daphnids for Scanning Electron Microscopy using hexamethyldisilazane. *Archiv für Hydrobiologie*, 149, 587–596

Lamed, R., Lobos, J.H., & Su, T.M. (1988). Effects of stirring and hydrogen on fermentation products of *Clostridium thermocellum*. *Applied and Environmental Microbiology, 54*, 1216 - 1221

Lamed, R., Setter, E., & Bayer, E. A. (1983). Characterization of a cellulose-binding, cellulase-

containing complex in *Clostridium thermocellum*. *Journal of Bacteriology*, *156*(2), 828–836. https://doi.org/10.1128/jb.156.2.828-836.1983

Lee, L. L., Crosby, J. R., Rubinstein, G. M., Laemthong, T., Bing, R. G., Straub, C. T., Adams, M. W. W., & Kelly, R. M. (2020). The biology and biotechnology of the genus *Caldicellulosiruptor*: recent developments in 'Caldi World.' *Extremophiles*, *24*(1), 1–15. https://doi.org/10.1007/s00792-019-01116-5

Levin, D., Islam, R., Cicek, N., & Sparling, R. (2006). Hydrogen production by *Clostridium thermocellum* 27405 from cellulosic biomass substrates. *International Journal of Hydrogen Energy*, *31*(11), 1496–1503. https://doi.org/10.1016/j.ijhydene.2006.06.015

Li, J., Yuan, H., & Yang, J. (2009). Bacteria and lignin degradation. *Front Biol China* 4:29–38. https://doi.org/10.1007/s11515-008-0097-8

Livak, K. J., & Schmittgen, T. D. (2001). Analysis of relative gene expression data using real-time quantitative PCR and the 2(-Delta Delta C(T)) Method. *Methods (San Diego, Calif.)*, *25*(4), 402–408. https://doi.org/10.1006/meth.2001.1262

Lo, J., Zheng, T., Hon, S., Olson, D. G., & Lynd, L. R. (2015). The bifunctional alcohol and aldehyde dehydrogenase gene, adhE, is necessary for ethanol production in *Clostridium thermocellum* and *Thermoanaerobacterium saccharolyticum*. *Journal of Bacteriology*, *197*(8), 1386–1393. https://doi.org/10.1128/jb.02450-14

Lu, Y., Zhang, Y.-H. P., & Lynd, L. R. (2006). Enzyme–microbe synergy during cellulose hydrolysis by *Clostridium thermocellum*. *Proceedings of the National Academy of Sciences*, *103*(44), 16165–16169. https://doi.org/10.1073/pnas.0605381103

Lynd, L. R., Grethlein, H. E., & Wolkin, R. H. (1989). Fermentation of cellulosic substrates in batch and continuous culture by *Clostridium thermocellum*. *Applied and Environmental Microbiology*, *55*(12), 3131–3139. https://doi.org/10.1128/aem.55.12.3131-3139.1989

Lynd, L.R., Liang, X., Biddy, M.J., Allee, A., Cai, H., Foust, T., Himmel, M.E., Laser, M.S., Wang, M., & Wyman, C.E. (2017). Cellulosic ethanol: status and innovation. *Curr Opin Biotechnol* 45:202–211. https://doi.org/10.1016/j.copbio.2017.03.008

Lynd, L.R., van Zyl, W.H., McBride, J.E., Laser, M. (2005). Consolidated bioprocessing of cellulosic biomass: an update. *Curr. Opin. Biotechnol*. 16, 577–583.

Lynd, L. R., Weimer, P. J., van Zyl, W. H., & Pretorius, I. S. (2002). Microbial cellulose utilization: fundamentals and biotechnology. *Microbiology and Molecular Biology Reviews*, *66*(4), 739–739. https://doi.org/10.1128/mmbr.66.4.739.2002

Marayuma, K. (1991). The discovery of adenosine triphosphate and the establishment of its structure. *Journal of the History of Biology*, *24*(1), 145–154. https://doi.org/10.1007/bf00130477

Mazzoli, R., Olson, D. G., & Lynd, L. R. (2020). Construction of lactic acid overproducing *Clostridium thermocellum* through enhancement of lactate dehydrogenase expression. *Enzyme and Microbial Technology*, *141*, 109645. https://doi.org/10.1016/j.enzmictec.2020.109645

McBee, R. H. (1954). The characteristics of *Clostridium thermocellum*. *Journal of Bacteriology*,

67(4), 505–506. https://doi.org/10.1128/jb.67.4.505-506.1954

McGovern, P. E., Zhang, J., Tang, J., Zhang, Z., Hall, G. R., Moreau, R. A., Nuñez, A., Butrym, E. D., Richards, M. P., Wang, C. S., Cheng, G., Zhao, Z., & Wang, C. (2004). Fermented beverages of pre- and proto-historic China. *Proceedings of the National Academy of Sciences of the United States of America*, *101*(51), 17593–17598. https://doi.org/10.1073/pnas.0407921102

Mertens, E., De Jonckheere, J., & Van Schaftingen, E. (1993). Pyrophosphate-dependent phosphofructokinase from the amoeba *Naegleria fowleri*, an AMP-sensitive enzyme. *Biochemical Journal*, *292*(3), 797–803. https://doi.org/10.1042/bj2920797

Myers, S., Zanobetti., A., Kloog, I., Huybers, P., Leakey, A.D.B., Bloom, A.J., Carlisle, E., Dietterich, L.H., Fitzgerald, G., Hasegawa, T., Holbrook., N.M., Nelson, R.L., Ottman, M.J., Raboy, V., Sakai, H., Sartor, K.A., Schwartz, J., Seneweera, S. and Tausz, M. and Usui, Y. (2014). Increasing CO_2 threatens human nutrition. *Nature*, Vol. 510 No. 7503, pp. 139-142

Nadkarni, M. A., Martin, F. E., Jacques, N. A., & Hunter, N. (2002). Determination of bacterial load by real-time PCR using a broad-range (universal) probe and primers set. *Microbiology (Reading, England)*, *148*(Pt 1), 257–266. https://doi.org/10.1099/00221287-148-1-257

Nozhevnikova, A. N., Russkova, Yu. I., Litti, Yu. V., Parshina, S. N., Zhuravleva, E. A., & Nikitina, A. A. (2020). Syntrophy and interspecies electron transfer in methanogenic microbial communities. *Microbiology*, *89*(2), 129–147. https://doi.org/10.1134/s0026261720020101

Olson, D. G., Hörl, M., Fuhrer, T., Cui, J., Zhou, J., Maloney, M. I., Amador-Noguez, D., Tian, L., Sauer, U., & Lynd, L. R. (2017). Glycolysis without pyruvate kinase in *Clostridium thermocellum*. *Metabolic Engineering*, *39*, 169–180. https://doi.org/10.1016/j.ymben.2016.11.011

Örlygsson, J., Anderson, R., & Svensson, B. H. (1995). Alanine as an end product during fermentation of monosaccharides by *Clostridium* strain P2. *Antonie van Leeuwenhoek*, *68*(4), 273–280. https://doi.org/10.1007/bf00874136

Ozkan, M., Desai, S., Zhang, Y., Stevenson, D., Beane, J., White, E., Guerinot, M., & Lynd, L. (2001). Characterization of 13 newly isolated strains of anaerobic, cellulolytic, thermophilic bacteria. *Journal of Industrial Microbiology and Biotechnology*, *27*(5), 275–280. https://doi.org/10.1038/sj.jim.7000082

Parisutham, V., Kim, T. H., & Lee, S. K. (2014). Feasibilities of consolidated bioprocessing microbes: from pretreatment to biofuel production. *Bioresource technology*, *161*, 431–440. https://doi.org/10.1016/j.biortech.2014.03.114

Prajapati, P., Varjani, S., Singhania, R. R., Patel, A. K., Awasthi, M. K., Sindhu, R., Zhang, Z., Binod, P., Awasthi, S. K., & Chaturvedi, P. (2021). Critical review on technological advancements for effective waste management of municipal solid waste: updates and way forward. *Environmental Technology & Innovation*, *23*, 101749. https://doi.org/10.1016/j.eti.2021.101749

Raman, B., McKeown, C.K., Rodriguez, M. Jr., Brown, S.D., Mielenz, J.R. (2011). Transcriptomic analysis of *Clostridium thermocellum* ATCC 27405 cellulose fermentation. *BMC Microbiol* 11:134

Rincon, M. T., Dassa, B., Flint, H. J., Travis, A. J., Jindou, S., Borovok, I., Lamed, R., Bayer, E. A., Henrissat, B., Coutinho, P. M., Antonopoulos, D. A., Berg Miller, M. E., & White, B. A. (2010). Abundance and diversity of dockerin-containing proteins in the fiber-degrading rumen bacterium, *Ruminococcus flavefaciens* FD-1. *PLoS ONE*, *5*(8), e12476. https://doi.org/10.1371/journal.pone.0012476

Roberts, S. B., Gowen, C. M., Brooks, J. P., & Fong, S. S. (2010). Genome-scale metabolic analysis of *Clostridium thermocellum* for bioethanol production. *BMC Systems Biology*, *4*(1). https://doi.org/10.1186/1752-0509-4-31

Robillard, C. M., Coristine, L. E., Soares, R. N., & Kerr, J. T. (2015). Facilitating climate-change-induced range shifts across continental land-use barriers. *Conservation Biology*, 29, 1586– 1595. https://doi-org.uml.idm.oclc.org/10.1111/cobi.12556

Russell, J. B., & Cook, G. M. (1995). Energetics of bacterial growth: Balance of anabolic and catabolic reactions. *Microbiological Reviews*, *59*(1), 48–62. https://doi.org/10.1128/mr.59.1.48-62.1995

Rydzak, T., Levin, D. B., Cicek, N., & Sparling, R. (2009). Growth phase-dependant enzyme profile of pyruvate catabolism and end-product formation in *Clostridium thermocellum* ATCC 27405. *Journal of Biotechnology*, *140*(3–4), 169–175. https://doi.org/10.1016/j.jbiotec.2009.01.022

Rydzak, T., McQueen, P., Krokhin, O.V., Spicer, V., Ezzati, P., Dwivedi, R.C., Shamshurin, D., Levin, D.B., Wilkins, J.A., & Sparling, R. (2012). Proteomic analysis of *Clostridium thermocellum* core metabolism: relative protein expression profiles and growth phase-dependent changes in protein expression. *BMC Microbiology, 12*, 214 - 214

Salimi, F., & Mahadevan, R. (2013). Characterizing metabolic interactions in a clostridial co-culture for consolidated bioprocessing. *BMC Biotechnology*, *13*(1). https://doi.org/10.1186/1472-6750-13-95

Sander, R. (2015). Compilation of Henry's law constants (version 4.0) for water as solvent. Atmos. Chem. Phys., 15, 4399–4981. doi:10.5194/acp-15-4399-2015

Schut, G. J., & Adams, M. W. W. (2009). The iron-hydrogenase of *Thermotoga maritima* utilizes ferredoxin and NADH synergistically: a new perspective on anaerobic hydrogen production. *Journal of Bacteriology*, *191*(13), 4451–4457. https://doi.org/10.1128/jb.01582-08

Soboh, B., Linder, D., & Hedderich, R. (2004). A multisubunit membrane-bound [NiFe] hydrogenase and an NADH-dependent Fe-only hydrogenase in the fermenting bacterium *Thermoanaerobacter tengcongensis*. *Microbiology*, *150*(7), 2451–2463. https://doi.org/10.1099/mic.0.27159-0

Solomon. (2010). Biofuels and sustainability. *Annals of the New York Academy of Sciences*, 1185(1), 119–134. https://doi.org/10.1111/j.1749-6632.2009.05279.x

Souza, G. M., Victoria, R. L., Joly, C. A., & Verdade, L. M. (2015). Bioenergy & sustainability: bridging the gaps. *SCOPE*, Paris.

Sparling, R., Islam, R., Cicek, N., Carere, C., Chow, H., & Levin, D. B. (2006). Formate synthesis by *Clostridium thermocellum* during anaerobic fermentation. *Canadian Journal of Microbiology*, *52*(7), 681–688. https://doi.org/10.1139/w06-021

Stams, A. J. M., & Plugge, C. M. (2009). Electron transfer in syntrophic communities of anaerobic bacteria and archaea. *Nature Reviews Microbiology*, *7*(8), 568–577. https://doi.org/10.1038/nrmicro2166

Strobel, H. J., Caldwell, F. C., & Dawson, K. A. (1995). Carbohydrate transport by the anaerobic thermophile *Clostridium thermocellum* LQRI. *Applied and Environmental Microbiology*, *61*(11), 4012–4015. https://doi.org/10.1128/aem.61.11.4012-4015.1995

Sun, S., Sun, S., Cao, X., & Sun, R. (2016). The role of pretreatment in improving the enzymatic hydrolysis of lignocellulosic materials. *Bioresource Technology*, *199*, 49–58. https://doi.org/10.1016/j.biortech.2015.08.061

Susskind, B. M., Warren, L. G., & Reeves, R. E. (1982). A pathway for the interconversion of hexose and pentose in the parasitic amoeba *Entamoeba histolytica*. *Biochemical Journal*, *204*(1), 191–199. https://doi.org/10.1042/bj2040191

Szech, U., Braun, M., & Kleiner, D. (1989). Uptake and excretion of amino acids by saccharolytic clostridia. *FEMS Microbiology Letters*, *58*(1), 11–14. https://doi.org/10.1111/j.1574-6968.1989.tb03009.x

Taillefer, M., Rydzak, T., Levin, D. B., Oresnik, I. J., & Sparling, R. (2015). Reassessment of the Transhydrogenase/Malate Shunt Pathway in *Clostridium thermocellum* ATCC 27405 through kinetic characterization of malic enzyme and malate dehydrogenase. *Applied and Environmental Microbiology*, *81*(7), 2423–2432. https://doi.org/10.1128/aem.03360-14

Taillefer, M., & Sparling, R. (2016). Glycolysis as the central core of fermentation. In *Advances in Biochemical Engineering/Biotechnology* (pp. 55–77). Springer International Publishing. http://dx.doi.org/10.1007/10_2015_5003

Thauer, R. K., Jungermann, K., & Decker, K. (1977). Energy conservation in chemotrophic anaerobic bacteria. *Bacteriological Reviews*, *41*(1), 100–180. https://doi.org/10.1128/br.41.1.100-180.1977

Thoma, C., Frank, M., Rachel, R., Schmid, S., Näther, D., Wanner, G., & Wirth, R. (2008). The Mth60 fimbriae of *Methanothermobacter thermoautotrophicus* are functional adhesins. *Environmental Microbiology*, *10*(10), 2785–2795. https://doi.org/10.1111/j.1462-2920.2008.01698.x

Thompson, R. A., & Trinh, C. T. (2017). Overflow metabolism and growth cessation in *Clostridium thermocellum* DSM1313 during high cellulose loading fermentations. *Biotechnology and Bioengineering*, *114*(11), 2592–2604. https://doi.org/10.1002/bit.26374

Tian, L., Papanek, B., Olson, D. G., Rydzak, T., Holwerda, E. K., Zheng, T., Zhou, J., Maloney,

M., Jiang, N., Giannone, R. J., Hettich, R. L., Guss, A. M., & Lynd, L. R. (2016). Simultaneous achievement of high ethanol yield and titer in *Clostridium thermocellum*. *Biotechnology for Biofuels*, *9*(1). https://doi.org/10.1186/s13068-016-0528-8

Tian, L., Perot, S. J., Hon, S., Zhou, J., Liang, X., Bouvier, J. T., Guss, A. M., Olson, D. G., & Lynd, L. R. (2017). Enhanced ethanol formation by *Clostridium thermocellum* via pyruvate decarboxylase. *Microbial Cell Factories*, *16*(1). https://doi.org/10.1186/s12934-017-0783-9

Tindall, B. J. (2019). The names *Hungateiclostridium* Zhang et al. 2018, *Hungateiclostridium thermocellum* (Viljoen et al. 1926) Zhang et al. 2018, *Hungateiclostridium cellulolyticum* (Patel et al. 1980) Zhang et al. 2018, *Hungateiclostridium aldrichii* (Yang et al. 1990) Zhang et al. 2018, *Hungateiclostridium alkalicellulosi* (Zhilina et al. 2006) Zhang et al. 2018, *Hungateiclostridium clariflavum* (Shiratori et al. 2009) Zhang et al. 2018, *Hungateiclostridium straminisolvens* (Kato et al. 2004) Zhang et al. 2018 and *Hungateiclostridium saccincola* (Koeck et al. 2016) Zhang et al. 2018 contravene Rule 51b of the International Code of Nomenclature of Prokaryotes and require replacement names in the genus *Acetivibrio* Patel et al. 1980. *International Journal of Systematic and Evolutionary Microbiology*, *69*(12), 3927–3932. https://doi.org/10.1099/ijsem.0.003685

Toni, L.S., Garcia, A.M., Jeffrey, D.A., Jiang, X., Stauffer, B.L., Miyamoto, S.D., & Sucharov, C.C. (2018). Optimization of phenol-chloroform RNA extraction. *MethodsX, 5*, 599 - 608.

U.S. Department of Energy. Making Cellulose More Accessible for Bioconversion. https://science.osti.gov/ber/Highlights/2014/BER-2014-07-p. Accessed 9 June 2022

van der Veen, D., Lo, J., Brown, S. D., Johnson, C. M., Tschaplinski, T. J., Martin, M., Engle, N. L., van den Berg, R. A., Argyros, A. D., Caiazza, N. C., Guss, A. M., & Lynd, L. R. (2013). Characterization of *Clostridium thermocellum* strains with disrupted fermentation end-product pathways. *Journal of Industrial Microbiology and Biotechnology*, *40*(7), 725–734. https://doi.org/10.1007/s10295-013-1275-5

Vazana, Y., Moraïs, S., Barak, Y., Lamed, R., & Bayer, E. A. (2010). Interplay between *Clostridium thermocellum* family 48 and family 9 cellulases in cellulosomal versus non-cellulosomal states. *Applied and Environmental Microbiology*, *76*(10), 3236–3243. https://doi.org/10.1128/aem.00009-10

Vignais, P., Billoud, B., & Meyer, J. (2001). Classification and phylogeny of hydrogenases. *FEMS Microbiology Reviews*, *25*(4), 455–501. https://doi.org/10.1016/s0168-6445(01)00063-8

Viljoen, J. A., Fred, E. B., & Peterson, W. H. (1926). The fermentation of cellulose by thermophilic bacteria. *The Journal of Agricultural Science*, *16*(1), 1–17. https://doi.org/10.1017/s0021859600088249

Vinuselvi, P., & Lee, S. K. (2012). Engineered *Escherichia coli* capable of co-utilization of cellobiose and xylose. *Enzyme and Microbial Technology*, *50*(1), 1–4. https://doi.org/10.1016/j.enzmictec.2011.10.001

Wang, H., Le, Y., & Sun, J. (2022). Light-driven bio-decolorization of triphenylmethane dyes by

a *Clostridium thermocellum*-CdS biohybrid. *Journal of hazardous materials*, *431*, 128596. Advance online publication. https://doi.org/10.1016/j.jhazmat.2022.128596

Wasserfallen, A., Nölling, J., Pfister, P., Reeve, J., & Conway de Macario, E. (2000). Phylogenetic analysis of 18 thermophilic *Methanobacterium* isolates supports the proposals to create a new genus, *Methanothermobacter* gen. nov., and to reclassify several isolates in three species, *Methanothermobacter thermautotrophicus* comb. nov., *Methanothermobacter wolfeii* comb. nov., and *Methanothermobacter marburgensis* sp. nov. *International Journal of Systematic and Evolutionary Microbiology*, *50*(1), 43–53. https://doi.org/10.1099/00207713-50-1-43

Weimer P.J. & Zeikus J.G. (1977). Fermentation of cellulose and cellobiose by *Clostridium thermocellum* in the absence and presence of *Methanobacterium thermoautotrophicum*. Applied and Environmental Microbiology, 33:289-297

WHO. (2008). Protecting Health From Climate Change: World Health Day 2008, World Health Organization, Geneva

Wolin, M.J. (1974). Metabolic interactions among intestinal microorganisms. *The American journal of clinical nutrition, 27 11*, 1320-8

Wrigley. E.A. (2013). Energy and the English Industrial Revolution. *Phil Trans R Soc A*, 371: 20110568. http://dx.doi.org/10.1098/rsta.2011.0568

Xu, Q., Singh, A., & Himmel, M. E. (2009). ChemInform abstract: perspectives and new directions for the production of bioethanol using consolidated bioprocessing of lignocellulose. *ChemInform*, *40*(49). https://doi.org/10.1002/chin.200949274

Yang, S.J., Kataeva, I., Wiegel, J., Yin, Y., Dam, P., Xu, Y., Westpheling, J., & Adams, M. W. W. (2010). Classification of '*Anaerocellum thermophilum*' strain DSM 6725 as *Caldicellulosiruptor bescii* sp. nov. *International Journal of Systematic and Evolutionary Microbiology*, *60*(9), 2011–2015. https://doi.org/10.1099/ijs.0.017731-0

Yayo, J., Kuil, T., Olson, D. G., Lynd, L. R., Holwerda, E. K., & van Maris, A. J. A. (2021). Laboratory evolution and reverse engineering of *Clostridium thermocellum* for growth on glucose and fructose. *Applied and Environmental Microbiology*, *87*(9). https://doi.org/10.1128/aem.03017-20

Yutin, N. and Galperin, M.Y. (2013). A genomic update on clostridial phylogeny: Gram-negative spore formers and other misplaced clostridia. *Environ Microbiol* 15:2631–2641. https://doi.org/10.1111/1462-2920.12173

Zhang, R. & Fujimori, S. (2020). The role of transport electrification in global climate change mitigation scenarios. *Environmental Research Letters*, Volume 15, Number 3

Zhang, Y.-H. P., & Lynd, L. R. (2005). Cellulose utilization by *Clostridium thermocellum*: bioenergetics and hydrolysis product assimilation. *Proceedings of the National Academy of Sciences*, *102*(20), 7321–7325. https://doi.org/10.1073/pnas.0408734102

Zhang, X., Tu, B., Dai, L., Lawson, PA., Zheng, Z., Liu, L-Y., Deng, Y., Zhang, H., and Cheng, L. (2018). *Petroclostridium xylanilyticum* gen. nov., sp. nov., a xylan- degrading bacterium isolated 173 from an oilfield, and reclassification of clostridial cluster III members into

four novel genera in a new *Hungateiclostridiaceae* fam. nov. Int J Syst Evol Microbiol 68:3197– 3211. https://doi.org/10.1099/ijsem.0.002966

Zhou, J., Olson, D. G., Argyros, D. A., Deng, Y., van Gulik, W. M., van Dijken, J. P., & Lynd, L. R. (2013). Atypical glycolysis in *Clostridium thermocellum*. *Applied and Environmental Microbiology*, *79*(9), 3000–3008. https://doi.org/10.1128/aem.04037-12

Zuroff, T. R., Xiques, S. B., & Curtis, W. R. (2013). Consortia-mediated bioprocessing of cellulose to ethanol with a symbiotic *Clostridium phytofermentans*/yeast co-culture. *Biotechnology for Biofuels*, *6*(1). https://doi.org/10.1186/1754-6834-6-59

Zverlov, V. V., Kellermann, J., & Schwarz, W. H. (2005). Functional sub-genomics of *Clostridium thermocellum* cellulosomal genes: identification of the major catalytic components in the extracellular complex and detection of three new enzymes. *PROTEOMICS*, *5*(14), 3646–3653. https://doi.org/10.1002/pmic.200401199